Static Crystal Effects on the Vibronic Structure of the Phosphorescence, Fluorescence, and Absorption Spectra of Benzene Isotopic Mixed Crystals

E. R. Bernstein, S. D. Colson, D. S. Tinti, and G. W. Robinson

Citation: The Journal of Chemical Physics **48**, 4632 (1968); doi: 10.1063/1.1668039
View online: http://dx.doi.org/10.1063/1.1668039
View Table of Contents: http://aip.scitation.org/toc/jcp/48/10
Published by the American Institute of Physics

differing by a factor of nearly 2. This is because[16] R_{2F}^0 is proportional to $\tau_c/(1+\omega_0^2\tau_c^2)$, and for $\omega_0^2\tau_c^2>1$ one has R_{2F}^0 proportional to $1/\omega_0^2$. However, the temperature dependence of R_{2F}^0 for neat 2-fluoropyridine, given in Table IV, is fitted well by a linear Arrhenius plot of positive slope, which corresponds to $\omega_0^2\tau_c^2<1$. Therefore, it appears that the differences between the two sets of data in Fig. 8 and Table V are mainly instrumental in origin. Further studies of such instrumental effects are needed. In the meantime it is germane that the exchange rate (R_{IN}) is less sensitive to error than is the magnitude of the corresponding, random time-dependent perturbation (J_{NF}). Moreover, if one wishes to make comparative studies of the latter, the relative instrumental errors can be reduced significantly by making all of the measurements on the same day, with the same spectrometer and the same instrumental settings.

THE JOURNAL OF CHEMICAL PHYSICS VOLUME 48, NUMBER 10 15 MAY 1968

Static Crystal Effects on the Vibronic Structure of the Phosphorescence, Fluorescence, and Absorption Spectra of Benzene Isotopic Mixed Crystals*

E. R. BERNSTEIN,† S. D. COLSON,‡ D. S. TINTI,§ AND G. W. ROBINSON

Gates and Crellin Laboratories of Chemistry,|| California Institute of Technology, Pasadena, California

(Received 7 December 1967)

The phosphorescence, fluorescence, and absorption spectra of the isotopic benzenes C_6H_6, C_6H_5D, p-$C_6H_4D_2$, and sym-$C_6H_3D_3$, present as dilute guests in a C_6D_6 host crystal at 4.2°K, are obtained with sufficient spectral resolution to ascertain the magnitude of the crystalline site effects. The relative vibronic intensities in fluorescence and phosphorescence are compared. Two site effects are emphasized: site splitting of degenerate fundamentals and orientational effects. The former can occur for the isotopes C_6H_6 and sym-$C_6H_3D_3$, while the latter is possible only for isotopes with less than a molecular threefold rotation axis. The observations show that both site-splitting and orientational effects do occur as a general rule on vibronic and vibrational states in benzene isotopic mixed crystals. An empirical correlation between the magnitudes of the site splitting, orientation effect and site (gas-to-crystal) shifts for in-plane and out-of-plane modes is noted. The phosphorescence of C_6H_6 and sym-$C_6H_3D_3$ has been completely analyzed out to 0, $0-(\nu_8+\nu_1)$, while for that of C_6D_5H the analysis of only the more intense bands near the electronic origin has been carried out. Some ground-state vibrations of p-$C_6H_4D_2$ are also presented but the phosphorescence spectrum, complicated greatly by both ground- and excited-state orientational effects, is not fully analyzed in the present work. Absorption spectra of these mixed crystals have yielded information concerning the orientational effect on the first excited singlet state of C_6H_5D and p-$C_6H_4D_2$ as well as site splitting of the ν_6' vibrational levels of C_6H_6. On heavily exposed photographic plates it has been possible to assign a number of transitions in the $^{13}CC_5H_6$ emission spectra. The $^{13}CC_5H_{6-n}D_n$ 0, 0 absorption spectra have also been identified. New absorptions, in the region of the 0, 0 transition of C_6H_6 and C_6H_5D have been tentatively assigned on the basis of their intensity behavior as a function of guest concentration to resonance-pair lines and to lines from $^{13}CC_5H_{6-n}D_n$ and $^{13}C_2C_4H_{6-n}D_n$.

I. INTRODUCTION

Since the classic work of Halford,[1] Hornig,[2] and Winston and Halford[3] in the late 1940's, the effect of the crystal environment on molecular spectra has been of much interest. This early research deals in part with the effect of the crystal site on degenerate molecular states. More recently, Bernstein[4] and Strizhevsky[5] have considered further site interactions not limited only to degenerate states, viz., orientational effects,[4] gas-to-crystal shifts,[4] and enhanced Fermi resonance[4,5] in the solid. For experimental as well as historical reasons, most of these investigations have concerned ground-state vibrations observable by means of infrared spectroscopy. Since it is of theoretical importance to know whether or not such effects are present for all the vi-

* Supported in part by the U.S. Air Force Office of Scientific Research.

† Present address: Department of Chemistry, University of Chicago, Chicago, Ill. 60637.

‡ Present address: Division of Pure Physics, National Research Council, Ottawa 7, Ontario, Canada.

§ Present address: Department of Chemistry, University of California at Los Angeles, Los Angeles, Calif. 90024.

|| Contribution No. 3546.

[1] R. S. Halford, J. Chem. Phys. **14**, 8 (1946).

[2] D. F. Hornig, J. Chem. Phys. **16**, 1063 (1948).

[3] H. Winston and R. S. Halford, J. Chem. Phys. **17**, 607 (1949).

[4] (a) E. R. Bernstein, "Site Effects in Isotopic Mixed Crystals—Site Shift, Site Splitting, Orientational Effect and Intermolecular Fermi Resonance in the Vibrational Spectrum of Benzene" (unpublished); (b) E. R. Bernstein and G. W. Robinson, "Vibrational Exciton Structure in Crystals of Isotopic Benzenes" (unpublished); (c) E. R. Bernstein, "Calculation of Ground State Vibrational Structure and Phonons of the Isotopic Benzene Crystals" (unpublished).

[5] V. L. Strizhevsky, Opt. Spektrosk. **8**, 165 (1960) [Opt. Spectrosc. **8**, 86 (1960)].

bration classes and types, in the present work we look for the above effects in the vibronic transitions of C_6H_6 and some of its deutereated isotopes. The phosphorescence, fluorescence, and absorption spectra of various benzene isotopic mixed crystals allow a study of site interactions in vibrations not seen in infrared absorption experiments.

For the case of a C_6H_6 guest in the C_i site[6] of a C_6D_6 host crystal, the molecular u, g classification of guest states is retained, imposing the $u \leftrightarrow g$ dipole selection rule for the C_6H_6 transitions. Thus, in the infrared absorption spectrum from the g ground state, only u vibrations are observed, while vibronic transitions involving u excited states can be utilized to study g vibrations. Electronic emission spectra therefore supplement vibrational data obtained from the Raman effect. On the other hand, in an isotope that does not have inversion symmetry, the infrared absorption and the ultraviolet emission can involve the same vibrations. It was because of these considerations that C_6H_6, C_6H_5D, *p*-$C_6H_4D_2$, and *sym*-$C_6H_3D_3$ were chosen for this work. These molecules were all studied as dilute guests in a C_6D_6 host crystal at 4.2°K. By such a study it is hoped that more can be learned about crystal effects on molecular vibrations with the aim of relating these effects to the intermolecular force fields present.

A vibrational analysis of the low-resolution benzene phosphorescence spectrum in EPA at 77°K was first published by Shull.[7] Sveshnikov and co-workers[8] and Leach and Lopez-Delgado[9] have compared the vibronic structure of phosphorescence and fluorescence in "glasses" at 77°K. Nieman[10] and Nieman and Tinti[11] have analyzed the benzene phosphorescence under moderate resolution for many benzene isotopes in a C_6D_6 host crystal at 4.2°K. The benzene emission spectra in amorphous solids do not generally show resolvable crystal effects on the ground-state vibrations. A few of these effects were observed in the crystal spectra of Nieman and Tinti, but it is only with the higher resolution employed here that the effects are discernible on nearly all vibronic bands and can be quantitatively discussed with confidence.

II. CRYSTAL EFFECTS ON MOLECULAR VIBRATIONS

Crystal effects on vibrations have been previously considered in great detail both in our laboratory and elsewhere. Site splitting[1,2] for a molecular energy state occurs if this level has a degenerate representation in the point group of the molecule that maps into one or more nondegenerate representations in the group of the crystal site. Thus, the doubly degenerate vibrations of C_6H_6 and *sym*-$C_6H_3D_3$ are mapped into two nondegenerate components in the C_i site of the benzene crystal. The energy difference between these two components in an "ideal mixed crystal" is defined as the site group splitting δ_s.[4,12] The concept of an "ideal mixed crystal" implies the absence of all resonance and quasiresonance intermolecular interactions, while all other interactions remain as in the pure crystal. Dilute ($<1\%$) isotopic mixed crystals of benzene have been shown to be an excellent approximation to the "ideal mixed crystal" for ground-state vibrations.[4] This is found not to be true, however, for the lowest excited electronic singlet state of benzene.[13]

For benzene isotopes without a molecular threefold axis, a different effect occurs.[4] It is clear that for C_6H_5D and *p*-$C_6H_4D_2$ in the C_i site there are three unique orientations with respect to rotation about the original sixfold axis. In principle, each orientation could have a different energy. Therefore, a molecular vibration in these molecules could give rise in the spectrum to three lines, each of which is due to a differently oriented molecule. For other site symmetries, a different number of physically distinct orientations is possible. Thus, the number of lines observed in the spectrum for a given vibration is an indication of the *effective* site symmetry. Table I summarizes the number of orientations theoretically possible for benzene isotopes in various sites.

TABLE I. Number of possible orientations for benzene isotopes in sites of different symmetries.

Molecule	Molecular symmetry	Site symmetry C_1	C_i	C_{2h}	D_{2h}
C_6H_6, C_6D_6	D_{6h}	1	1	1	1
sym-$C_6H_3D_3$	D_{3h}	2	1	1	1
p-$C_6H_4D_2$	D_{2h}	3	3	3[a], 2	2
C_6H_5D, *o*-$C_6H_4D_2$, *m*-$C_6H_4D_2$, *vic*-$C_6H_3D_3$	C_{2v}	6	3	3[a], 2	2
asym-$C_6H_3D_3$	C_s	12	6	6[a], 3	3

[a] Plane of the site same as the molecular plane.

[6] E. G. Cox, Rev. Mod. Phys. **30**, 159 (1958); E. G. Cox, D. W. J. Cruickshank, and J. A. S. Smith, Proc. Roy. Soc. (London) **A247**, 1 (1958).

[7] H. Shull, J. Chem. Phys. **17**, 295 (1949).

[8] B. Ya. Sveshnikov and P. P. Dikun, Dokl. Akad. Nauk SSSR **65**, 637 (1949); Zh. Eksp. Teor. Fiz. **19**, 1000 (1949); T. V. Ivanova and B. Ya. Sveshnikov, Opt. Spektrosk. **11**, 598 (1961) [Opt. Spectrosc. **11**, 322 (1961)].

[9] S. Leach and R. Lopez-Delgado, J. Chim. Phys. **61**, 1636 (1964).

[10] G. C. Nieman, Ph.D. thesis, California Institute of Technology, 1965.

[11] G. C. Nieman and D. S. Tinti, J. Chem. Phys. **46**, 1432 (1967).

[12] E. R. Bernstein, S. D. Colson, R. Kopelman, and G. W. Robinson, "Electronic and Vibrational Exciton Structure in Crystalline Benzene," J. Chem. Phys. (to be published).

[13] S. D. Colson, "Location of the Fourth, Forbidden Factor Group Component of the $^1B_{2u}$ State of Crystalline Benzene," J. Chem. Phys. (to be published).

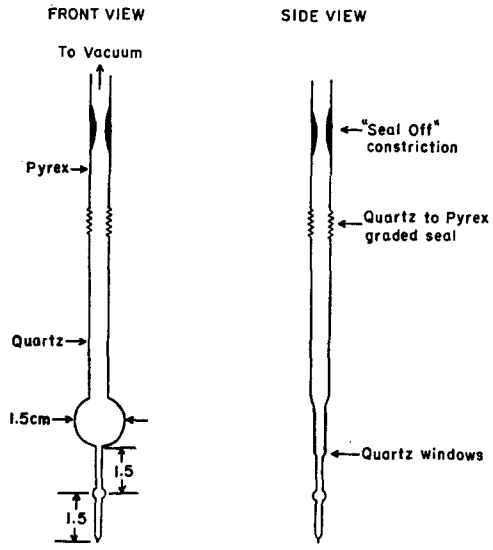

FIG. 1. Modified "Bridgman-type" sample cell.

III. EXPERIMENTAL

The benzenes were obtained from Merck, Sharp & Dohme, Ltd., of Montreal, Canada. The mixed isotopic solutions were purified by the method described by Colson and Bernstein[14] and directly vacuum distilled into modified "Bridgman-type" growing tubes like that depicted in Fig. 1. Two thicknesses of crystal were used: 3 mm and $\sim 20\ \mu$. The thick crystals were grown by lowering the optical cells through a temperature gradient of about 100°C/cm directly into a liquid-N_2-cooled chamber at the rate of roughly 1 cm/day. These crystals, which are usually transparent and nearly free of cracks, are then cooled to 4.2°K with little decrease in quality. This same technique has been successful in growing crystals up to 3 cm in length. The thin crystals are grown in the same type tube by suspending the holder in a Dewar approximately 20 cm above the liquid-N_2 surface and subsequently cooling to helium temperatures. Once the crystal holder is completely submerged under the liquid helium, the cell is broken open above the graded seal to insure good thermal contact with the coolant. If this is not done, the sample temperature has been found to remain well above 4.2°K for some length of time, and in addition temperature increases occur when the sample is irradiated.

Both high- and low-pressure Hg lamps were employed as excitation sources. The emission spectra of the guest were excited by absorbing into the C_6D_6 host singlet exciton band from which the excitation energy is rapidly transferred to the lowest excited singlet and triplet states of the guest. These states lie approximately 30 cm^{-1} to lower energy than the corresponding state of the C_6D_6 host for each hydrogen atom substituted. The guests thus serve as effective energy traps from which emission is observed at low temperatures.

The phosphorescence spectra of the mixed isotopic crystals were photographed at 4.2°K on a Jarrell-Ash 3.4-m Ebert spectrograph. Two gratings were employed. The first had a ruling of 15 000 lines/in., yielding a plate factor of roughly 1.62 Å/mm in the third order. Exposure times for the more intense vibronic lines were about 5 min with 20-μ entrance slits. The weaker lines required approximately 1-h exposures. A second grating was used in the 18th order where the plate factor was 0.32 Å/mm. Only the more intense vibronic lines of C_6H_6 were photographed with this grating. Exposure times of 4 h were required with 40-μ entrance slits.

All fluorescence and some of the survey phosphorescence spectra were obtained on a 2.0-m Czerny-Turner spectrograph, constructed in our laboratory, with a 15 000-lines/in. grating blazed at 1.0 μ. Spectra were usually taken in the second and third orders (plate factors 3.7 and 2.4 Å/mm) for the phosphorescence and fluorescence regions, respectively. Exposure times for 5-μ slits were roughly 5 min. Some of the very weak phosphorescence lines were measured from these plates.

Absorption spectra were taken on the 3.4-m instrument utilizing the fourth order of the lower resolution grating, which gives a plate factor of roughly 1.23 Å/mm at 2650 Å. A few spectra were also photographed with the higher-resolution grating.

Order sorting, where necessary, was accomplished by Kasha[15] liquid filters or Corning glass filters in conjunction with 0.1-m·atm Cl_2 and Br_2 filters. When the high orders were used, a small Bausch & Lomb monochrometer was used as a predispersing element or, on its side, as an order sorter.

IV. EMISSION SPECTRA

A. Phosphorescence Lifetimes

Exposure times for the more intense features in the phosphorescence and fluorescence spectra are roughly equal at lower dispersions, implying nearly equal quantum yields for the singlet and triplet emissions of the guest molecule. Furthermore, the measured phosphorescence lifetimes of the guests C_6H_6, C_6H_5D, p-$C_6H_4D_2$, and sym-$C_6H_3D_3$ are independent of the isotopic composition of the guest. The lifetimes are also independent of concentration in the low-concentration ($\lesssim 1\%$) range. The phosphorescence intensity, followed over the first decade change for individual vibronic lines, decays exponentially (within experimental error) with an average lifetime of 8.7 sec (see Table II). This constant triplet lifetime implies that the quantum yields are approximately independent of isotopic substitu-

[14] S. D. Colson and E. R. Bernstein, J. Chem. Phys. **43**, 2661 (1965).

[15] M. Kasha, J. Opt. Soc. Am. **38**, 11, 929 (1948).

tion in the guest. The lack of a strong isotope effect[16] except near the limit of complete deuteration has also been reported by Martin and Kalantar[17] for benzene in various low-temperature organic glasses. These authors have attributed this behavior to the dominant activity of the "totally symmetric C–H stretching mode" in the $^3B_{1u} \nrightarrow {}^1A_{1g}$ nonradiative transition. They have reasoned that since there is only one such mode for all the partially protonated benzenes, additional hydrogen atoms beyond the first have little effect on the nonradiative transition probability. Because of resonance effects in the crystal, our lifetime measurements cannot be carried very close to the perdeutero limit, but our observation of little isotope effect on overall lifetime for the four molecules studied is entirely consistent with the more extensive findings of Martin and Kalantar.

B. Linewidths

The phosphorescence consists of somewhat sharper lines and is thus easier to photograph at higher dispersion. Due to this smaller linewidth and the greater wavenumber dispersion available in the phosphorescence spectral region, we have concentrated mainly on the phosphorescence spectrum as a means of studying ground-state vibrations. The larger of the site splittings to be discussed here are resolved in both fluorescence and phosphorescence. We have used the fluorescence to complement the phosphorescence where possible.

The narrowest phosphorescence linewidth at the highest resolution employed is approximately 0.1 cm^{-1} and seems to be limited by the quality of the crystal. This linewidth was observed only once in a very transparent, seemingly near perfect, crystal of 0.04% C_6H_6 in C_6D_6. The linewidth of 0.1 cm^{-1} was superimposed on a weaker background whose width was approximately 0.5 cm^{-1}. This latter width probably corresponds to residual crystal imperfections. It should be noted that the narrowest linewidth we obtained roughly equals the expected zero-field splitting in the triplet state. It is also comparable to the instrumental resolution. Since the final states in these sharp emission spectra are low-lying excited vibrational levels of the ground electronic state, the observation implies that the vibrational relaxation times from these states are $\gtrsim 0.5 \times 10^{-10}$ sec.

TABLE II. Phosphorescence lifetime of isotopically mixed benzene crystals at 4.2°K.

Host	Guest	Weight % guest	τ[a] (sec)
C_6D_6	C_6H_6	0.82	8.7
		0.093	8.5
		0.014	8.7
C_6D_6	C_6H_5D	0.94	8.5
		0.15	8.5
		0.013	8.6
C_6D_6	*p*-$C_6H_4D_2$	0.86	8.6
		0.16	8.9
		0.016	8.9
C_6D_6	*sym*-$C_6H_3D_3$	1.05	8.7
		0.22	8.3
		0.0088	9.0
sym-$C_6H_3D_3$	C_6H_6	0.009	8.4

[a] ±0.2 sec.

[16] G. W. Robinson, J. Mol. Spectry. **6**, 58 (1961).
[17] T. E. Martin and A. H. Kalantar (unpublished results).

C. Vibronic Selection Rules

The lowest triplet state of C_6H_6 most likely has B_{1u} symmetry in point group D_{6h}.[18] It is thus both spin and electronically forbidden. This double forbiddenness in the free molecule can be formally removed in a second-order perturbation scheme by some combination of spin–orbit and vibronic mixing. The three spin–orbit states of the vibrationless level of the $^3B_{1u}$ state of C_6H_6 form bases for the irreducible representations E_{2u} and B_{2u} of the D_{6h} point group. These three levels, providing they are populated, can undergo dipole transitions with a variety of excited vibrational levels in the electronic ground state: $E_{2u} \rightarrow b_{1g}$, b_{2g}, e_{1g} (in-plane polarized); $E_{2u} \rightarrow e_{2g}$ (out-of-plane polarized); $B_{2u} \rightarrow e_{2g}$ (in-plane polarized); $B_{2u} \rightarrow b_{1g}$ (out-of-plane polarized). Since C_6H_6 has no b_{1g} fundamental, higher-order vibronic coupling would be required (see Sec. 4b, Ref. 19), and consequently b_{1g} vibrations are not expected to occur with much intensity in the spectrum.

For the lowest excited benzene singlet state,[19] B_{2u} symmetry in point group D_{6h} has been established with greater certainty than the triplet symmetry. The spatial forbiddenness of the transition between the ground $^1A_{1g}$ state and the lowest excited $^1B_{2u}$ state can be formally removed by vibronic mixing of the $^1B_{2u}$ state with the dipole allowed $^1E_{1u}$ and $^1A_{2u}$ states. The latter route requires a b_{1g} fundamental of which benzene has none. However, e_{2g} vibrations can mix B_{2u} and E_{1u} states. Thus, vibrations of species e_{2g} are group theoretically predicted to be active in the fluorescence and singlet absorption spectra. Vibronic calculations[20] predict that the e_{2g} vibration ν_6 should dominate.[21]

In the C_i site of the C_6D_6 host crystal, only the *g*, *u* classification of molecular states is retained, and,

[18] See, however, G. Castro and R. M. Hochstrasser, J. Chem. Phys. **46**, 3617 (1967), who suggest that the lowest triplet may be $^3B_{2u}$.
[19] J. H. Callomon, T. M. Dunn and I. M. Mills, Phil. Trans. Roy. Soc. London **A259**, 499 (1966).
[20] A. C. Albrecht, J. Chem. Phys. **33**, 156, 169 (1960); D. P. Craig, J. Chem. Soc. **1950**, 2146; J. N. Murrell and J. A. Pople, Proc. Phys. Soc. (London) **A69**, 641 (1961).
[21] Here and elsewhere in this work, the normal coordinates are numbered after E. B. Wilson, J. C. Decius, and P. C. Cross, *Molecular Vibrations* (McGraw-Hill Book Co., New York, 1955).

therefore, the above group-theoretical arguments are no longer rigorously correct. However, it is found experimentally (*vide infra*) that the above scheme predicts the dominant features of the spectrum, implying that the molecular classification of states is still approximately valid. The effect of the site is demonstrated by the appearance in both the fluorescence and phosphorescence of a totally symmetric progression built on a relatively weak 0, 0 band.

D. Phonons

One feature common to both emissions is the activity of a 72-cm^{-1} lattice phonon. The phonon emission band is quite broad ($\sim$5 cm^{-1}) and is observed only for the stronger molecular bands. A phonon of the same frequency is also found in the pure crystal absorption spectrum.[13] On heavily exposed, lower dispersion plates of the emission spectra, the phonon band is shaded to lower energy, and this shading extends nearly to the "zero-phonon" vibronic line. Some additional structure appears within this shaded region and also weakly to higher-energy of the 72-cm^{-1} peak.

The value of the phonon frequency is apparently determined mainly by the properties of the bulk crystal, independent of the actual guest, since the frequency does not change measurably for different isotopic guests. This result is in agreement with the optical phonons observed in the Raman effect at 4.2°K,[22] where 62- and 77-cm^{-1} phonons are observed for C_6D_6 and 69- and 86-cm^{-1} phonons for C_6H_6. Some unobserved optical phonons are also estimated[4c,22] to have very similar frequencies, and again show little change between C_6H_6 and C_6D_6. The nature of the 72-cm^{-1} phonon (or phonons) is not known, but symmetry requires that it be a *gerade* type.

E. Discussion of the Spectra

1. C_6H_6

Figure 2 shows a microphotometer tracing of the phosphorescence spectrum of C_6H_6 out to 0, 0–2500 cm^{-1}. The analysis of the C_6H_6 phosphorescence is given in Table III for frequencies less than that corresponding to $(\nu_8+\nu_1)$, while Table IV summarizes the frequencies and numbering of the fundamentals of C_6H_6 in gas, liquid, and crystal phases; the latter values are derived from the analysis presented in Table III and from the infrared spectrum[4] of C_6H_6 in a C_6D_6 host. Table V compares the relative intensity of the stronger vibronic origins in the C_6H_6 phosphorescence and fluorescence spectra as determined from microphotometer tracings of photographic plates.

The most active vibrations in the phosphorescence spectrum of C_6H_6 in a C_6D_6 host are the same as previously assigned in solid glasses. However, the occurrence of much sharper lines in the mixed-crystal spectra allows a more nearly complete and unambiguous analysis. For example, some of the fundamentals of $^{13}C^{12}C_5H_6$ can be assigned (*vide infra*). C_6H_6 has four degenerate fundamentals of e_{2g} symmetry—ν_6, ν_7, ν_8, and ν_9. Figure 2 and Tables III and V show the general dominance of e_{2g} vibrations, in particular of ν_8 and ν_9, in activating the triplet emission spectrum. This observation is in qualitative agreement with the results of vibronic theory.[20] The almost exclusive activation of the C_6H_6 phosphorescence by the modes ν_8 and ν_9 is carried over to all the lower-symmetry isotopes. The only e_{2g} fundamental not assigned in the phosphorescence is ν_7.

Progressions of the totally symmetric 990-cm^{-1} (a_{1g}, ν_1) vibration on all the observed fundamental, combination, and overtone vibrations are present. The fundamental ν_6 by itself is quite weak. However, when in combination with ν_1 it steals intensity from ν_8 by Fermi resonance. The totally symmetric progression built on the $\nu_{10}(e_{1g})$ origin is the weakest progression analyzed, being weaker than some progressions based on combinations or overtones of u fundamentals having overall symmetry e_{2g}.

The only g fundamentals that have not been assigned in the phosphorescence of C_6H_6 are $\nu_2(a_{1g})$, $\nu_3(a_{2g})$, and $\nu_7(e_{2g})$. However, ν_2 and ν_7 are assigned from the fluorescence spectrum. No u vibrations are seen in either emission.

Many of the same ground-state vibrations are observed in the fluorescence spectrum as in the phosphorescence. However, the relative vibronic activity is substantially different, as can be seen from Table V. The relative intensities in the fluorescence also agree generally with the qualitative predictions of vibronic theory. In comparing the two emissions the following features seem noteworthy. The b_{2g} modes, both fundamentals and combinations, are relatively much more intense in the phosphorescence. The only b_{2g} mode we have assigned in the fluorescence is the fundamental ν_4, which appears very weakly. No vibrations of species b_{2g} have been seen in the gas-phase $^1B_{2u}$–$^1A_{1g}$ spectrum.[19] The presence of a b_{2g} vibronic origin in the free molecule would support a B_{1u} assignment for the lowest singlet state, but in the crystal the presence of the extremely weak b_{2g} origin could easily be caused by crystal site interactions.

The intensity of the totally symmetric fundamental ν_1 relative to the most intense vibronic origin is much greater in the fluorescence than in the phosphorescence, implying a greater environmental enhancement of the 0, 0 transition in fluorescence.

Site splitting δ_s is observed for the degenerate e_{2g} fundamentals ν_6, ν_7, and ν_9 amounting to 3.1, 5.5, and 0.54 cm^{-1}, respectively. See Figs. 2 and 3 and Table III. The splitting of ν_9 is seen only with the highest resolution employed and is not shown in Table III. Figure 3 depicts a densitometer tracing of ν_9 and ν_8 with this highest resolution. Curiously no distinct site splitting

[22] M. Ito and T. Shigeoka, Spectrochim. Acta **22**, 1029 (1966).

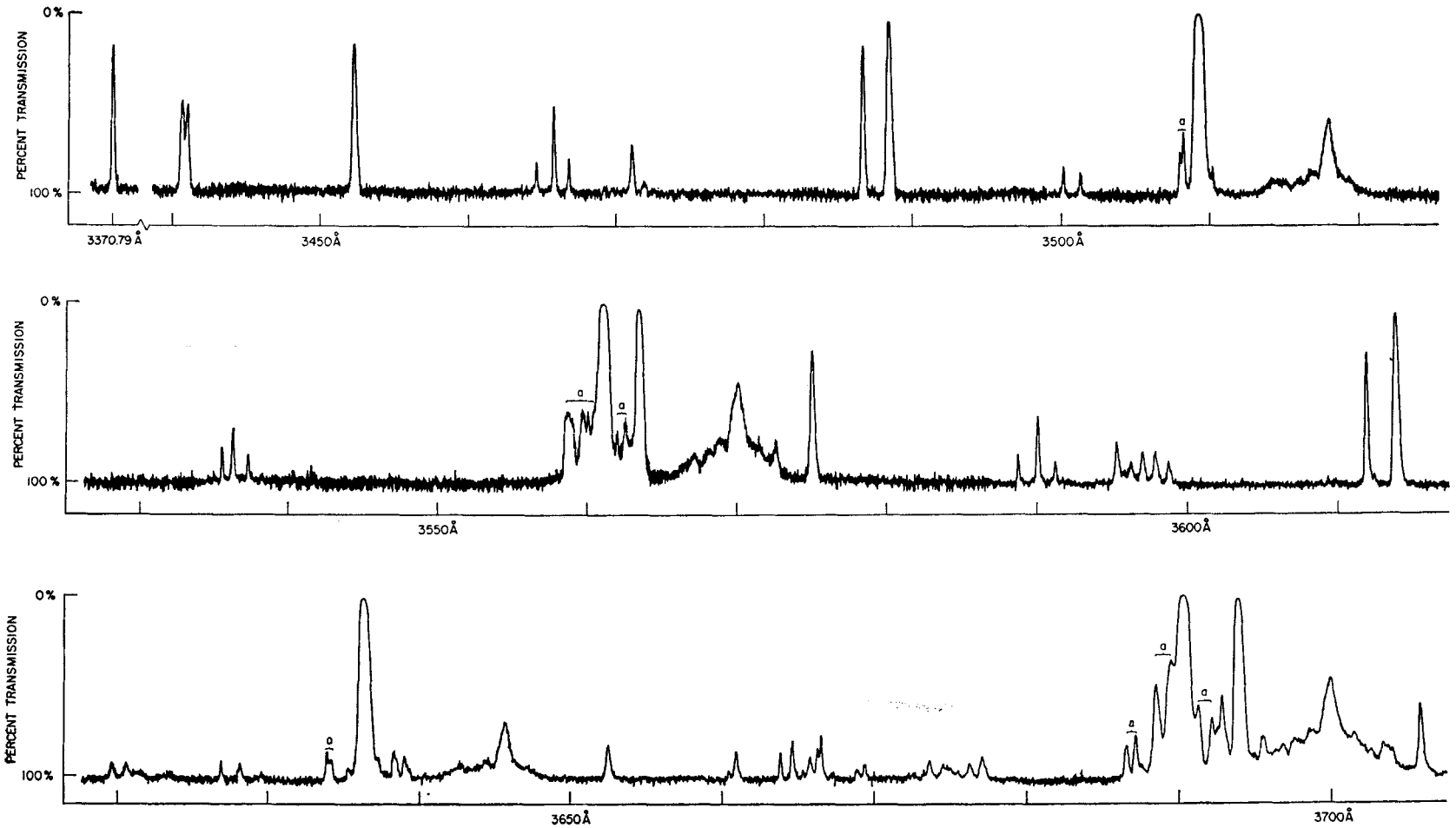

FIG. 2. Microphotometer tracing of a lower resolution plate of the C_6H_6 phosphosescence. The bands labeled "a" are due to $^{13}C^{12}C_5H_6$ and discussed in the text.

TABLE III. Analysis of the C_6H_6 phosphorescence.

λ_{air} (Å)	ν_{vac} (cm^{-1})	Relative intensity	$\Delta\nu$ (cm^{-1})	Assignment[a]	Vibrational symmetry in D_{6h}	Predicted harmonic value (cm^{-1})
3369.90	29 666.0	vvw		^{13}C 0, 0		
70.79	658.2	m	0	0, 0		
3441.13	051.9	mw	606.3	ν_6	e_{1g}	
41.49	048.8	mw	609.4			
52.85	28 953.3	m	704.9	ν_4	b_{1g}	
65.22	849.9	w	808.3			809.6
66.40	840.1	mw	818.1	$2\nu_{16}$	$e_{2g}+a_{1g}$	817.8
67.45	831.4	w	826.8			826.0
71.75	795.7	w	862.5	ν_{10}	e_{1g}	
72.57	788.9	vw	869.3			
87.25	667.7	m	990.5	ν_1	a_{1g}	
87.90	662.4	vw	995.8	$^{13}C\nu_5$		
89.00	653.3	s	1004.9	ν_5	b_{2g}	
3500.82	556.6	w	1101.6	$\nu_{11}+\nu_{16}$	e_{2g}	1101.7
01.96	547.3	w	1110.9			1109.9
08.58	493.4	w	1164.8	$^{13}C\ \nu_{9,a\ b}$		
08.83	491.4	w	1166.8			
09.79	483.6	vs	1174.6	ν_9	e_{2g}	
10.84	475.1	vw	1183.1	?		
18.63	412.0	w, b	1246.2	$\nu_9+71.6$		
3535.51	28 276.4	w	1381.8			1383.1
36.21	270.8	mw	1387.4	$\nu_{16}+\nu_{17}$	$e_{2g}+a_{2g}+a_{1g}$	1387.5
36.8	266.	vw	1392.			1391.3
37.25	262.5	w	1395.7			1395.7
58.53	093.4	mw	1564.8			
59.01	089.6	mw	1568.6	^{13}C ?		
59.65	084.6	mw, b	1573.6			
60.43	078.4	mw, b	1579.8			
61.00	073.9	vs	1584.3	ν_8	e_{2g}	
62.56	061.7	mw, b	1596.5	^{13}C ?		
63.35	055.4	s	1602.8	$\nu_6+\nu_1$	e_{2g}	1596.8
63.51	054.2	s	1604.0			1599.9
64.32	047.8	vw	1610.4	$\nu_6+\nu_5$	e_{1g}	1611.2
64.52	046.2	vw	1612.0			1614.3
70.10	002.4	w, b	1655.8	$\nu_8+71.5$		
72.59	27 982.9	w, b	1675.3	$\nu_6+\nu_1+71.3$		

TABLE III. (*Continued*)

λ_{air} (Å)	ν_{vac} (cm^{-1})	Relative intensity	$\Delta\nu$ (cm^{-1})	Assignment[a]	Vibrational symmetry in D_{6h}	Predicted harmonic[b] value (cm^{-1})
74.99	964.1	m	1694.1	$\nu_4+\nu_1$	b_{2g}	1695.4
88.75	856.9	w	1801.3	$2\nu_{16}+\nu_1$	$e_{2g}+a_{1g}$	1800.1
90.08	846.5	mw	1811.7			1808.3
91.20	837.9	w	1820.3			1816.5
95.31	806.0	w	1852.2	$\nu_{10}+\nu_1$	e_{1g}	1853.0
96.24	798.8	vw, b	1859.4			1859.8
3597.02	27 792.8	w	1865.4	$\nu_{10}+\nu_5$	e_{2g}	1867.4
97.86	786.3	w	1871.9			1874.2
98.77	779.3	w	1878.9	$\nu_9+\nu_4$	e_{1g}	1879.5
3611.63	680.4	vw, sh	1977.8	$^{13}C\ \nu_5+\nu_1$		
11.89	678.4	m	1979.8	$2\nu_1$	a_{1g}	1981.0
12.42	674.4	vw	1983.8	?		
13.78	664.0	s	1994.2	$\nu_5+\nu_1$	b_{2g}	1995.4
19.30	621.8	w	2036.4	$\nu_{10}+\nu_9$	$e_{1g}+b_{2g}+b_{1g}$	2037.1
20.35	613.8	w	2044.4			2043.9
26.75	565.1	w	2093.1	$\nu_{11}+\nu_{16}+\nu_1$	e_{2g}	2092.2
28.00	555.6	w	2102.6			2100.4
29.39	545.0	vw	2113.2	?		
33.76	511.8	w	2146.4	$^{13}C\ \nu_{9a,\ b}+\nu_1$		
34.05	509.6	w	2148.6			
35.32	500.0	vw	2158.2	$\nu_{12}+\nu_{15}$?	a_{2g}	2158.2
36.13	493.9	vs	2164.3	$\nu_9+\nu_1$	e_{2g}	2165.1
37.23	485.6	vw	2172.6	?		
38.20	478.3	w	2179.9	$\nu_9+\nu_5$	e_{1g}	2179.5
38.35	477.1	w, sh	2181.0	$\nu_{15}+\nu_{18}$	e_{2g}	2181.7
38.90	473.0	w	2185.2			2185.5
45.57	422.7	w, b	2235.5	$\nu_9+\nu_1+71.2$		
52.47	370.9	w	2287.3	$\nu_8+\nu_4$	e_{1g}	2289.2
3660.46	27 311.2	vw	2347.0	$\nu_{14}+\nu_{18}$	e_{2g}	2347.4
60.98	307.3	w	2350.9			2351.2
63.87	285.8	w	2372.4	$\nu_{16}+\nu_{17}+\nu_1$	$e_{2g}+a_{1g}+a_{1g}$	2373.6
64.65	280.0	w	2378.2			2378.0
65.31	275.1	vw	2383.1			2381.8
65.83	271.2	w, b	2387.0	$2\nu_6+\nu_9$	$2e_{2g}+a_{2g}+a_{1g}$	2386.2, 2387.2
66.31	267.6	w	2390.6			2390.3
66.53	266.0	w	2392.2			2393.4

TABLE III. (*Continued*)

λ_{air} (Å)	ν_{vac} (cm^{-1})	Relative intensity	$\Delta\nu$ (cm^{-1})	Assignment[a]	Vibrational symmetry in D_{6h}	Predicted harmonic value (cm^{-1})
68.94	248.1	w	2410.1	?		
69.46	244.2	w	2414.0	?		
73.73	212.5	w	2445.7	$\nu_8+\nu_{10}$	$e_{1g}+b_{2g}+b_{1g}$	2446.8
74.58	206.2	w, b	2452.0			2453.6
76.39	192.8	w	2465.4	$\nu_6+\nu_1+\nu_{10}$	$e_{1g}+b_{2g}+b_{1g}$	2465.9
77.15	187.2	w, b	2471.0			2472.7
86.68	116.9	mw	2541.3	^{13}C ?		
87.24	112.8	mw	2545.4			
88.60	102.8	m	2555.4			
89.58	095.6	m	2562.6			
90.34	090.1	vs	2568.1	$\nu_8+\nu_1$	e_{2g}	2574.8
91.38	082.4	mw	2575.8	^{13}C ?		
92.27	075.9	mw	2582.3			
93.00	070.6	mw	2587.6	$\nu_8+\nu_5$	e_{1g}	2589.2
3693.91	27 063.9	s	2594.3	$\nu_6+2\nu_1$	e_{2g}	2587.3
94.07	062.7	s	2595.5			2590.4
95.54	052.0	vw	2606.2	$\nu_6+\nu_1+\nu_5$	e_{1g}	2601.7
95.70	050.8	vw	2607.4			2604.8
3700.06	018.9	w, b	2639.3	$\nu_8+\nu_1+71.2$		
05.92	26 976.2	mw	2682.0	$\nu_4+2\nu_1$	b_{2g}	2685.9

[a] Bands in Fermi resonance are connected by brackets.

occurs for ν_8, but, as seen in Fig. 3, the ν_8 linewidth is only a little less than the total width of the split ν_9 fundamental and might represent an unresolved site splitting.

A very weak line, which has not been assigned, is observed $\sim$8.5 cm^{-1} to the low-energy side of the very strong 0, $0-\nu_9-n\nu_1$ progression. The intensity ratio of ν_9 to the unassigned line is >100, much larger than the intensity ratio ($\lesssim 10$) for the two components of any other observed site-split fundamental. We thus feel that this weak feature does not represent the other component of ν_9.

The e_{1g} fundamental ν_{10} is also split ($\delta_s=6.8$ cm^{-1}). In the observed combinations of ν_{10} with $\nu_5(e_{1g}\times b_{2g}=e_{2g})$ and with ν_9, ν_8 and $\nu_6+\nu_1$ ($e_{1g}\times e_{2g}=b_{1g}+b_{2g}+e_{1g}$) only doublets are observed with the ν_{10} fundamental splitting repeating itself. The intensities of the two site components belonging to the ν_{10} fundamental are quite different (see weak lines near 3472 Å in Fig. 2) but tend to equalize in the combinations. For the totally symmetric progression built on ν_{10} the intensity difference remains. The mode ν_{10} is not observed in the fluorescence, apparently since it has e_{1g} symmetry in D_{6h}, but the overtone $2\nu_{10}(e_{2g})$ is seen very weakly, and a site splitting of 7 cm^{-1} can be inferred. Thus, even though the vibronic intensities of the site-split components of ν_{10} in the phosphorescence are widely different, and the reason for this difference is not understood, the reported site splitting and the frequencies of the components must certainly be correct.

In the combination and overtone vibronic bands, site splitting in many u fundamentals can be inferred. Consider for example the three lines at 808.3, 818.1, and 826.8 cm^{-1}, which are assigned as $2\nu_{16}$, $(e_{2u})^2=e_{2g}+a_{1g}$ in D_{6h}. Both site and intramolecular anharmonic terms can remove the threefold degeneracy of the $2\nu_{16}$ overtone. If the anharmonic terms dominated, the splitting would not be symmetric. However, if the

TABLE IV. Summary of C_6H_6 data (cm^{-1}).

D_{6h} symmetry class	Vibration number and type[a]	Fundamental frequency			Site splitting
		Gas[b]	Liquid[c]	Crystal[d]	
a_{1g}	ν_1 (CC)	995.4	(993)	990.5	
	ν_2 (CH)	(3073)	(3062)	3063.3	
a_{2g}	ν_3 ($H^{\parallel}$)	(1350)	1346		
b_{2g}	ν_4 ($C^{\perp}$)	(707)	(707)	704.9	
	ν_5 ($H^{\perp}$)	(990)	(991)	1004.9	
e_{2g}	ν_6 ($C^{\parallel}$)	608.0	(606)	606.3, 609.4	3.1
	ν_7 (CH)	(3056)	(3048)	3042.0, 3047.5	5.5
	ν_8 (CC)[e]	(1590)	1586	1584.2	≤ 0.3
	ν_9 ($H^{\parallel}$)	(1178)	1177	1174.3_4, 1174.8_8	0.5_4
e_{1g}	ν_{10} ($H^{\perp}$)	(846)	850	862.5, 869.3	6.8
a_{2u}	ν_{11} ($H^{\perp}$)	674.0	675	696.9 [697]	
b_{1u}	ν_{12} ($C^{\parallel}$)	(1010)	1010	1011.3 [1011]	
	ν_{13} (CH)	(3057)	(3048)		
b_{2u}	ν_{14} (CC)	(1309)	1309	1312.6 [1313]	
	ν_{15} ($H^{\parallel}$)	(1146)	1146	1146.9 [1147]	
e_{2u}	ν_{16} ($C^{\perp}$)	398.6	404	404.8, 413.0 [404, 413]	8.2
	ν_{17} ($H^{\perp}$)	(967)	969	978.3, 983.9 [978, 983]	5.6
e_{1u}	ν_{18} ($H^{\parallel}$)	1037	1035	1034.8, 1038.6 [1034, 1038]	3.8
	ν_{19} (CC)	1482	1479		
	ν_{20} (CH)[e]	3047	3036		

[a] The vibrational numbering for this and the other isotopes follows Refs. 21 and 28.

[b] Taken from summary given in Ref. 28. Parentheses indicate calculated values.

[c] Reference 19.

[d] The frequencies of the u fundamentals are from Ref. 4. The values inferred from the uv spectra, rounded off to the nearest cm^{-1}, are given in brackets and are of course less accurate.

[e] Uncorrected for Fermi resonance.

fundamental ν_{16} were split in the site, then the overtone would be expected to consist of three symmetrically spaced lines with intensities determined by the binomial coefficients 1:2:1 (assuming equal vibronic activity among the three components). As can be seen from Fig. 2 and Table III the intensities in the phosphorescence are roughly in this ratio and the splitting is very nearly symmetrical. The two site split components of the e_{2u} fundamental ν_{16} are therefore predicted to occur at 404.2 and 413.0 cm^{-1} with a site splitting δ_s of 8.8 cm^{-1}. In the infrared spectrum of C_6H_6 in a C_6D_6 host crystal,[4] ν_{16} consists of a doublet at 404.8 and 413.0 cm^{-1} ($\delta_s = 8.2$ cm^{-1}) in excellent agreement with the values inferred from the electronic emission spectra. Deviations from the simple pattern might be expected not only because of intramolecular anharmonicities but also because of vibronic effects and possible Fermi resonance among the trio of lines each of which rigorously has only symmetry a_g in the C_i site. The same vibration observed in the fluorescence, for instance, does not show the 1:2:1 intensity pattern, the high-energy component at 827 cm^{-1} being more intense relative to the other two.

The doublet at 1101.6 and 1110.9 cm^{-1}, which is assigned to $\nu_{11}+\nu_{16}$, is the combination of ν_{11} with each of the site-split components of ν_{16}. Assuming no anharmonic corrections or resonances, the inferred value of ν_{11} is 697.4 cm^{-1}, which compares with 696.9 observed in the infrared.

Applying the ν_{16} infrared frequencies 404.8 and 413.0 cm^{-1} to the quartet assigned to $\nu_{16}+\nu_{17}$ at about 1390 cm^{-1} yields for the degenerate fundamental ν_{17} the frequencies 978.0 and 982.7 cm^{-1}. This analysis gives an inferred site splitting of 4.7 cm^{-1} for ν_{17}, which should

TABLE V. Relative intensity estimates for the stronger vibronic origins in the C_6H_6 phosphorescence and fluorescence spectra.

Symmetry	Vibration	$^3B_{1u}\rightarrow{}^1A_{1g}$	$^1B_{2u}\rightarrow{}^1A_{1g}$
e_{2g}	ν_6	1	100
	ν_7	...	3
	ν_8[a]	100	20
	ν_9	25	3
	$2\nu_{16}$	1	3
	$\nu_{11}+\nu_{16}$	<1	5
b_{2g}	ν_4	1	<1
	ν_5	6	...
a_{1g}	0, 0	1	b
	ν_1	1	22
	ν_2	...	1
e_{1g}	ν_{10}	<1	...

[a] Uncorrected for Fermi resonance with $\nu_6+\nu_1$.
[b] Because of appreciable reabsorption, no relative intensity estimate is given.

be compared with 5.6 cm^{-1} directly observed in the infrared. The observed ν_{17} infrared lines occur at 978.3 and 983.9 cm^{-1} (see Table IV).

In summary, it is seen from Table IV that 16 of the 20 benzene fundamentals are now accurately known from mixed crystal infrared and electronic emission spectra. The site splittings for eight of the 10 degenerate fundamentals have also been established.

2. $^{13}C^{12}C_5H_6$

The isotope ^{13}C is present in natural abundance in the amount of 1.1%. Thus, roughly 6.6% of any benzene will contain at least one ^{13}C atom. For the partially deuterated benzenes, more than one species with the chemical formula $^{13}C^{12}C_5H_nD_{6-n}$ exists. The corresponding vibrational frequencies of each of these isotopes will be very similar and difficult to resolve. However, only one isomer of $^{13}C^{12}C_5H_6$ exists and the electronic spectra provide a means of obtaining some of the vibrational frequencies of $^{13}C^{12}C_5H_6$ as an "impurity" in the C_6H_6 guest in the C_6D_6 crystal. This technique may have a definite advantage over conventional infrared spectroscopy for studying ^{13}C benzene in natural abundance since in an electronic transition the separation between corresponding vibronic lines depends not only on the vibrational energy difference but also on a relatively large zero-point energy contribution. Even if a particular vibrational frequency were unchanged by introducing ^{13}C, the corresponding vibronic lines will still be separated in energy by this zero-point effect.

In actuality, however, the electronic emission spectra have been only of limited usefulness for studying ^{13}C-benzene vibrations for several reasons. Although ~6% of the isotopic guest is ^{13}C benzene, the ^{13}C-to-^{12}C phosphorescence intensity ratio is less than 6%. The reason for this is that the *electronic* transition energy for ^{13}C benzene lies above that of ^{12}C benzene, and at low temperatures excitation energy transfer to the lowest lying trap, i.e., the ^{12}C benzene, can reduce the relative intensity of emission from the ^{13}C isotope. Definitive assignments of all but the more intense ^{13}C lines are further hampered by the intense background of ^{12}C lines and their associated phonon structure on heavily exposed plates.

Since $^{13}C^{12}C_5H_6$ has vibrational symmetry C_{2v}, the vibrations degenerate in D_{6h} are split into *a* and *b* components. In the C_i site the vibrations of $^{13}C^{12}C_5H_6$ can be further perturbed by orientational effects and thus give rise to further apparent splittings or line broadening. However, the orientation effects caused by one ^{13}C atom should be much smaller than that for one D atom, since the guest–host interaction is more sensitive to changes on the periphery of the interacting molecules. The orientation effects for C_6H_5D, discussed in a following section, are in general $\lesssim 1$ cm^{-1} and thus are expected to be vanishingly small for $^{13}C^{12}C_5H_6$. Therefore, the only new vibrational structure anticipated is from the removal of the vibrational degeneracies.

A somewhat surprising result for $^{13}C^{12}C_5H_6$ is that the isotope shifts in the electronic origins of the phosphorescence and fluorescence are quite different, contrary to the observations for the deuterium substituted isotopes.[11,23] These shifts to high energy from the corresponding C_6H_6 transitions are 3.6 and 7.8 cm^{-1} in the $^1B_{2u}$–$^1A_{1g}$ and $^3B_{1u}$–$^1A_{1g}$ 0, 0 lines, respectively. The electronic origin in the singlet transition, as will be discussed in Sec. V, is determined from the 0, 0 line

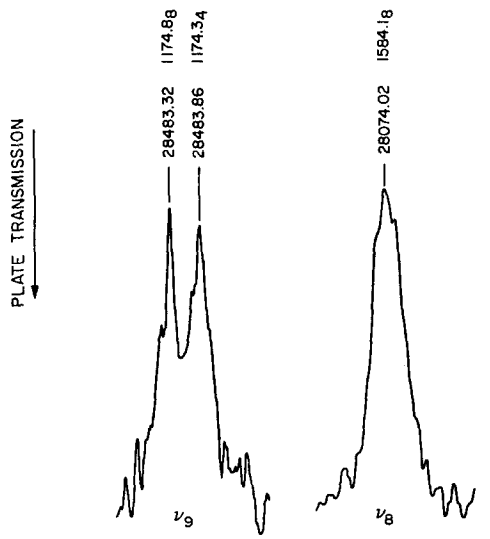

FIG. 3. Microphotometer tracing of the 0, 0—ν_9 and 0, 0—ν_9 C_6H_6 phosphorescence lines at the highest resolution employed.

[23] F. M. Garforth, C. K. Ingold, and H. G. Poole, J. Chem. Soc. 1948, 508.

observed in absorption. The assignment is confirmed by the presence in the fluorescence spectrum of $^{13}C^{12}C_5H_6$ of a progression built on this origin involving the known fundamental[24,25] ν_1 of species a_1. The mixed crystal value observed for this fundamental is 982.0 cm^{-1} compared to the liquid value[24] of 984 cm^{-1}.

The other $^{13}C^{12}CH_6$ fundamentals assigned with some certainty are ν_4, ν_5, ν_{9a}, and ν_{9b}. These were obtained from the phosphorescence, wherein they serve as origins for progressions in ν_1. The 0, 0 and 0, 0-ν_4 lines are very weak and were photographed only with the faster, lower-resolution instrument. The bands involving $\nu_{9a,b}$ are seen in Fig. 2 as weak doublets just to the short-wavelength side of the very strong 0, 0-ν_9-$n\nu_1$ progression of C_6H_6. The progressions built on ν_4 and ν_5 are too weak to see on an exposure corresponding to Fig. 2, as is the 0, 0 transition. The fundamental frequencies of $^{13}C^{12}C_5H_6$ are presented in Table VI. The observed ^{13}C shifts are also tabulated and compared with the shift calculated from Whiffen's[26] force field employing the modifications of Albrecht.[27] The agreement between the predicted and observed shifts for the fundamentals ν_1, ν_4, ν_5, and $\nu_{9a,b}$ is excellent and generally within the experimental error limits of ± 0.3 cm^{-1}. This range is imposed mainly by the uncertainty in the phosphorescence electronic origin. The ^{13}C vibronic lines terminating in the ground-state fundamentals are nearly as sharp as the C_6H_6 lines at the same resolution, confirming our expectations of a very small orientation effect for $^{13}C^{12}C_5H_6$.

Other lines are observed in both fluorescence and phosphorescence that are perhaps associated with ^{13}C benzene, but the analysis leaves some doubt. For example, ν_6 is expected to be stronger than ν_1 in fluorescence (cf., Table V). A single line of about the correct intensity relative to ν_6 of ^{12}C benzene is seen 599.5 cm^{-1} from the ^{13}C 0, 0 line. If the $\nu_{6a,b}$ splitting is greater than about 5 cm^{-1} and if the low-energy component is the one observed, the other component of ν_6 would be unresolved from the overexposed ν_6 band of ^{12}C benzene. Two very weak lines are seen in the phosphorescence spectrum at 600 and 606 cm^{-1} from the ^{13}C 0, 0 and thus seemingly support the assignment to $\nu_{6a,b}$. However, this analysis cannot be confirmed by a progression of ν_1 built on $\nu_{6a,b}$. Moderately intense lines are seen in the correct spectral region in both the fluorescence and phosphorescence emissions, but they are not easily assigned to $\nu_{6a,b}+\nu_1$. Because of the different ^{13}C shifts in the phosphorescence and fluorescence electronic origins, the ^{13}C lines are shifted relative to the ^{12}C lines in the two emissions. Some lines show the correct shift, but a sufficient number do not or are absent. We therefore consider the assignment of these lines tentative at best. Moreover, $\nu_{6a,b,b}+\nu_1$ is most likely in Fermi resonance with $\nu_{8a,b}$ and possibly also with $\nu_{6a,b}+\nu_{12}$. Therefore, we do not speculate on an assignment for $\nu_{8a,b}$, even though in the phosphorescence it is expected to be stronger than the assigned $\nu_{9a,b}$.

TABLE VI. Some observed and calculated fundamental frequencies of $^{13}C^{12}C_5H_6$.

$^{13}C^{12}C_5H_6$ fundamental		$\Delta\nu(^{12}C-^{13}C)$	
Frequency	(cm^{-1})[a]	Observed[b]	Predicted[c]
ν_1	982.0	8.5	8.4
ν_4	702.0	2.9	3.5
ν_5	1003.8	1.1	1.0
$\nu_{9a,b}$	1174.6	0.0	0.3
	1172.6	2.0	2.4

[a] The experimental error is ± 0.3 cm^{-1}.
[b] The mean of the site-split fundamental ν_9 of $^{12}C_6H_6$ was used to calculate the $\Delta\nu$ observed.
[c] See text.

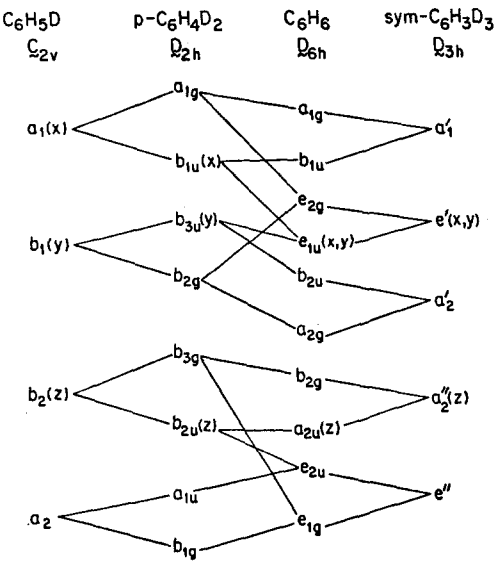

FIG. 4. Correlation diagram for the groups of benzene isotopes. The z axis is always perpendicular to the plane of the molecule; the y axis through C_1 (carbon atom one); and the x axis between C_2 and C_3. The irreducible representations b_{1g} in $\mathbf{D}_{6h}$ and a_1'' in $\mathbf{D}_{3h}$ do not correspond to any fundamental vibrations and are therefore omitted from the figure.

For the other $^{13}C^{12}C_5H_nD_{6-n}$ isotopes, which are, of course, present in the deuterated benzenes, no assignments to ^{13}C benzene are made. However, some of the unassigned weak lines, especially in the spectrum of *sym*-$C_6H_3D_3$, could easily be due to $^{13}C^{12}CC_5H_3D_3$.

3. *sym*-$C_6H_3D_3$

From the correlation diagram shown in Fig. 4, the active vibrations in the phosphorescence of *sym*-$C_6H_3D_3$

[24] A. Longseth and R. C. Lord, Jr., J. Chem. Phys. **38**, 203 (1938).
[25] A. R. Gee and G. W. Robinson, J. Chem. Phys. **46**, 4847 (1967).
[26] D. H. Whiffen, Phil. Trans. Roy. Soc. London **A248**, 131 (1955).
[27] A. C. Albrecht, J. Mol. Spectry. **5**, 236 (1960).

(point group D_{3h}) are predicted to have symmetry a_2'', e', and e''. However, only vibrations that correlate directly with the active C_6H_6 vibrations—ν_4, ν_5, ν_6, ν_8, and ν_9—or those that are strongly mixed with them in the lower-symmetry isotope give intense vibronic origins in the phosphorescence. For the mixing to be strong the vibrations must have similar frequencies and the same symmetry in point group D_{3h} of the free molecule. Thus, as shown by the normal coordinate analysis of Brodersen and Langseth,[28] relatively strong mixing occurs between ν_9 and ν_{18}, between ν_4 and ν_{11}, and between ν_8 and ν_{19}. Weaker mixing does occur to some extent among all vibrations of the same symmetry, and in the C_i site mixing is formally allowed among *all* the vibrations of *sym*-$C_6H_3D_3$. This latter mixing, however, does not appear to be very strong since the vibrations predicted to be active from the C_6H_6 spectrum are the more intense. Figure 5 shows a microphotometer tracing of the phosphorescence spectrum of sym-$C_6H_3D_3$ in crystalline C_6D_6 near the electronic origin. All of the observed fundamentals serve as "false origins" for totally symmetric $\nu_1(a_1', 955\ cm^{-1})$ and $\nu_{12}(a_1', 1003\ cm^{-1})$ progressions. The analysis of the sym-$C_6H_3D_3$ phosphorescence out to 0, 0-$(\nu_8+\nu_1)$ is given in Table VII. Some of the lines shown in Fig. 5 are known to be due to *m*-$C_6H_4D_2$ and *m*-$C_6H_2D_4$ impurities, having been identified from the phosphorescence spectrum of these isotopes in a C_6D_6 host. These frequencies are not included in Table VII. The possibility that some of the unassigned lines might be due to isotopic impurities other than the two above has not been investigated.

The vibrational degeneracies in *sym*-$C_6H_3D_3$, as in C_6H_6, can also be removed by the low-symmetry crystalline field, giving rise to site splittings. Nine of the 10 degenerate vibrations have been assigned from the phosphorescence and fluorescence spectra. Site splitting is directly observed on four e' and two e'' fundamentals and inferred for the third e'' fundamental. $\nu_{20}(e')$ was obtained from the fluorescence spectrum. Because of the difficulty in obtaining sharp lines in the fluorescence, the site splitting in ν_{20} could be as large as 3 cm^{-1} and not be resolved. For $\nu_{19}(e')$ the site splitting is probably less than 1 cm^{-1} since only one line was observed. The results are summarized in Table VIII.

None of the three possible a_2' vibrations—ν_3, ν_{14}, and ν_{15}—could be detected in the emission spectra. These were observed in the infrared spectrum of *sym*-$C_6H_3D_3$ in both C_6H_6 and C_6D_6 hosts.[4] For the ground-state fundamentals that do occur both in the infrared spectrum and in the electronic emission spectrum, the measured frequencies agree within experimental error except for the case of ν_{17}. The site-split components of the fundamental ν_{17} in the phosphorescence have quite different intensities, the high-energy component being usually too weak to be observed in most combinations. The two components are seen only in ν_{17} and in the doublets tentatively assigned to $\nu_{17}+\nu_5$, where the splitting repeats itself but the intensities become more nearly equal. This behavior is similar to ν_{10} in both C_6H_6 and *sym*-$C_6H_3D_3$, but for ν_{17} the intensity difference is greater. The more intense component of ν_{17} at 936.7 cm^{-1} agrees with one of the infrared values using a C_6D_6 host, but the weaker component at 940.7 cm^{-1} differs from the other infrared value by $\sim$2 cm^{-1}. This difference would seem to lie outside the combined experimental errors. Furthermore, the infrared values for the *sym*-$C_6H_3D_3$ ν_{17} vibration in the two hosts C_6H_6 and C_6D_6 show larger than usual shifts ($\sim$1 cm^{-1}), but this borders on the reported experimental error. Considering the weakness of the high-energy component in the phosphorescence, the assignment to ν_{17} may be questioned. However, if this is not the correct assignment, then the vibronic intensity of the second component of ν_{17} must be undetectably weak, considering that its position is known from the mixed crystal infrared spectrum, where ν_{17} is observed to be a distinct doublet.

An alternate assignment of the 940.7-cm^{-1} component would be ν_1 of either or both of the two $^{13}C^{12}C_5H_3D_3$ species present. Brodersen and Langseth[28] have assigned a Raman line at 947 cm^{-1}, observed in liquid *sym*-$C_6H_3D_3$, to $^{13}C^{12}C_5H_3D_3$. If the ^{13}C-isotope zero-point energy shift is roughly equal to 7.8 cm^{-1}, as for $^{13}C^{12}C_5H_6$, then application of this shift to 940.7 cm^{-1} gives near agreement with the Brodersen and Langseth value. Because of problems with the ν_{17} assignment and the existence of this reasonable alternate assignment, we consider the interpretation in Table VIII of the 940.7-cm^{-1} line to be quite tentative.

At $\Delta\nu\approx$1100 cm^{-1} the fundamental $\nu_9(e')$ is very likely in resonance with the combination $\nu_{10}+\nu_{16}(e'+a_1'+a_2')$. The ν_9 fundamental is expected to be strong in the phosphorescence, and the two strongest lines in this region are found to be degenerate with two of the harmonic values for $\nu_{10}+\nu_{16}$. Six lines in all are observed, the ν_9 component of the Fermi multiplet apparently being responsible for most of the intensity in the two intense components, and $\nu_{10}+\nu_{16}$ being responsible for the appearance of the other four lines. However, unambiguous assignments cannot be made. Similar problems occur at $\Delta\nu\approx$2270 cm^{-1}. The fundamental ν_7 is expected to occur in this region, but again overlapping combinations make a unique assignment difficult, especially from the phosphorescence spectrum alone (see Table VII). However, in the *sym*-$C_6H_3D_3$ fluorescence, the relative vibronic intensity of ν_7 is increased and the lines richest in ν_7 stand out more clearly. These lines occur at 2269.0 and 2274 cm^{-1}.

Of course, the higher the energy of the ground-state vibration, the more severe the problems with Fermi resonance become. Furthermore, for all the isotopes the emission lines become broader with higher vibrational energy, and an underlying continuum appears.

[28] S. Brodersen and A. Langseth, Kgl. Danske Videnskab. Selskab, Mat.-Fys. Skrifter **1**, No. 1 (1956).

TABLE VII. Analysis of the *sym*-$C_6H_3D_3$ phosphorescence.

λ_{air} (Å)	ν_{vac} (cm^{-1})	Relative intensity	$\Delta\nu$ (cm^{-1})	Assignment[a]	Vibrational symmetry in D_{3h}	Predicted harmonic value[b] (cm^{-1})
3361.89	29 753.8	m	0			
3422.78	29 207.6	m	546.2	ν_{11}	a_2''	
28.14	162.0	m	591.8	ν_6	e'	
28.33	160.3	m	593.5			
41.33	050.2	m	703.9	ν_4	a_2''	
43.06	035.6	mw	718.2	ν_{10}	e''	
43.59	031.1	vw	722.7			
47.55	28 997.8	w	756.0			
48.65	988.6	mw	765.2	$2\nu_{16}$	$a_1'+e'$	
49.70	979.7	w	774.1			
56.55	922.3	ms	831.5	ν_{18}	e'	
56.97	918.8	ms	835.0			
68.10	825.9	m	927.9	ν_5	a_2''	
69.17	817.1	mw	936.7	ν_{17}	e''	
69.66	813.1	vvw	940.7			
71.33	799.2	m	954.6	ν_1	a_1'	
77.15	750.9	mw	1002.9	ν_{12}	a_1'	
86.06	677.5	m	1076.3	$\nu_4+\nu_{16}$?	e'	1081.9
86.80	671.3	ms	1082.5			1090.9
87.89	662.4	vw	1091.4	$2\nu_{11}$?	a_1'	1092.4
3488.02	28 661.4	vw	1092.4	?		
88.35	658.6	m	1095.2			
88.60	656.5	m	1097.3			
88.99	653.4	ms	1100.4	ν_9	e'	
89.35	650.4	ms	1103.4	$\nu_{10}+\nu_{16}$	$e'+a_1'+a_2'$	
89.65	848.0	m	1105.8			
90.19	643.5	vw	1110.3			
3508.92	490.6	mw	1263.2	$\nu_{11}+\nu_{10}$	e'	1263.0
09.46	486.3	mw	1267.5			1267.5
14.70	443.8	vw	1310.0			
15.22	439.6	w	1314.2	$\nu_{16}+\nu_5$,	e'	
15.44	437.8	vw	1316.0	$\nu_{10}+\nu_6$,	$e''+a_1''+a_2''$	
15.97	433.5	vw	1320.3	$\nu_{16}+\nu_{17}$	$e'+a_1'+a_2'$	
16.88	426.2	vw	1327.6			
27.23	342.8	ms	1411.0	ν_{19}	e'	

TABLE VII. (*Continued*)

λ_{air} (Å)	ν_{vac} (cm^{-1})	Relative intensity	$\Delta\nu$ (cm^{-1})	Assignment[a]	Vibrational symmetry in D_{3h}	Predicted harmonic value (cm^{-1})
28.63	331.5	mw	1422.3	$\nu_6+\nu_{18}$	$e'+a_1'+a_2'$	
29.02	328.3	w	1425.5			
29.52	324.4	m	1429.4	$\nu_4+\nu_{10}$	e'	
35.07	279.9	vvw	1473.9	$\nu_{11}+\nu_5$	a'	1474.1
36.18	271.0	vvw	1482.8	$\nu_{11}+\nu_{17}$	e'	1482.9
38.32	253.9	mw	1499.9	$\nu_{11}+\nu_1$	a_2''	1500.8
3542.63	28 219.5	w	1534.3	?		
43.90	209.5	s	1544.3	$\nu_6+\nu_1$	e'	1546.5
44.13	207.6	s	1546.2			1548.2
44.67	203.3	w	1550.5	$\nu_{11}+\nu_{12}$	a_2''	1549.1
45.00	200.7	mw	1553.1	$\nu_{18}+\nu_{10}$?	$e''+a_1''+a_2''$	
45.98	192.9	m	1560.9	?		
46.43	189.3	w	1564.5	?		
47.28	182.6	vs	1571.2	ν_8[b]	e'	
47.41	181.6	vs	1572.2			
48.39	173.7	w	1580.1	?		
49.12	168.0	vw	1585.8	?		
56.44	110	m, vb	1644	ν_8+72		
57.24	103.6	w	1650.2	$\nu_5+\nu_{10}$?	e'	1646.0
57.82	099.1	vw	1654.7			1650.5
58.22	095.9	mw	1657.9	$\nu_4+\nu_1$	a_2''	1658.5
60.09	081.2	w	1672.6	$\nu_{10}+\nu_1$	e''	1672.8
60.68	076.5	vw	1677.3			1677.3
61.01	073.9	w	1679.9	?		
64.26	048.3	w	1705.5	$\nu_4+\nu_{12}$	a_2''	1706.8
65.09	041.8	w	1712.0	$2\nu_{16}+\nu_1$	$a_1'+e'$	1710.6
66.29	032.3	mw	1721.5			1719.8
67.42	023.5	w	1730.3			1728.7
3570.96	27 995.7	vvw	1758.1	$2\nu_{16}+\nu_{12}$	$a_1'+e'$	1758.9
72.14	986.4	vw	1767.4			1768.1
73.28	977.5	vvw	1776.3			1777.0
74.54	967.6	m	1786.2	$\nu_{18}+\nu_1$	e'	1786.1
75.00	964.0	m	1789.8			1789.2
80.71	919.6	mw	1834.2	$\nu_{18}+\nu_{12}$	e'	1834.4
81.14	916.1	mw	1837.7			1837.5
83.19	899.9	vw	1853.9	$2\nu_5$?	a_1'	1855.8

TABLE VII. (*Continued*)

λ_{air} (Å)	ν_{vac} (cm^{-1})	Relative intensity	$\Delta\nu$ (cm^{-1})	Assignment[a]	Vibrational symmetry in D_{3h}	Predicted harmonic value (cm^{-1})
84.27	891.7	vw	1862.1	$\nu_5+\nu_{17}$	e'	1864.5
84.93	886.6	vw	1867.2			1868.6
86.83	871.8	m	1882.0	$\nu_5+\nu_1$	a_2''	1882.4
87.97	863.0	w	1890.8	$\nu_{17}+\nu_1$	e''	1891.3
90.45	845.3	w	1908.5	$2\nu_1$	a_1'	1909.2
93.05	823.5	mw	1930.3	$\nu_5+\nu_{12}$	a_2''	1930.8
94.18	814.8	vw	1939.0	$\nu_{17}+\nu_{12}$	e''	1939.5
96.52	796.7	w	1957.1	$\nu_{12}+\nu_1$	a_1'	1957.5
3604.60	734.4	vvw	2019.4	?		
06.13	722.6	mw	2031.2	$\nu_4+\nu_{16}+\nu_1$?	e'	2036.0
06.91	716.6	m	2037.2			2043.5
08.03	708.0	vvw	2045.8	?		
3608.59	27 703.7	mw	2050.1			
08.88	701.5	mw	2052.3			
09.27	698.8	m	2055.0	$\nu_9+\nu_1$	e'	
09.67	695.8	m	2058.0	$\nu_{10}+\nu_{16}+\nu_1$	$e'+a_1'+a_2'$	
09.92	693.5	m	2060.3			
12.23	675.8	vw	2078.0	$\nu_4+\nu_{16}+\nu_{12}$?	e'	2084.8
13.08	669.3	w	2084.5			2093.8
13.74	664.3	vvw	2089.5	?		
14.12	661.4	vw	2092.4	?		
14.62	657.5	vvw	2096.3			
14.95	655.0	vvw	2098.8	$\nu_9+\nu_{12}$	e'	
15.45	651.2	w	2102.6			
15.80	648.5	mw	2105.3	$\nu_{10}+\nu_{16}+\nu_{12}$	$e'+a_1'+a_2'$	
16.05	646.6	w	2107.2			
17.42	636.1	vvw	2117.7	?		
23.59	589.1	vvw	2164.7	?		
24.33	583.4	vvw	2170.4	?		
26.60	566.2	vvw	2187.6	?		
27.37	560.3	vvw	2193.5	?		
28.83	549.2	vvw	2205.6	?		
3630.37	27 537.6	w	2216.2	$\nu_{11}+\nu_{10}+\nu_1$	e'	2219.0
30.93	533.3	vw	2220.5			2223.5

TABLE VII. (*Continued*)

λ_{air} (Å)	ν_{vac} (cm^{-1})	Relative intensity	$\Delta\nu$ (cm^{-1})	Assignment[a]	Vibrational symmetry in D_{3h}	Predicted harmonic value (cm^{-1})
36.21	493.3	vvw	2260.5			
36.69	489.7	vw	2264.1	$\nu_{11}+\nu_{10}+\nu_{12}$; $\nu_{10}+\nu_6+\nu_1$		
37.32	484.9	w	2268.9	ν_7; $\nu_{16}+\nu_5+\nu_1$		
38.09	479.1	w, b	2274.4	$\nu_8+\nu_4$; $\nu_{16}+\nu_{17}+\nu_1$		
39.14	471.2	vw	2282.6	ν_{13}		
40.08	464.1	w, b	2289.7			
40.64	459.9	w, b	2293.9	$\nu_8+\nu_{10}$	$e''+a_1''+a_2''$	
41.80	451.1	vw	2302.7			
43.14	441.1	vw, b	2312.7			
44.41	431.5	vvw	2322.3	$\nu_6+\nu_{12}+\nu_{14}$		
44.97	427.2	vvw	2326.6	$2\nu_{16}+\nu_{12}+\nu_{11}$		
45.93	420.0	vvw	2333.8	$2\nu_{16}+\nu_8$		
47.40	409.0	w	2344.6	$\nu_{19}+\nu_{17}$		
47.55	407.1	w	2346.6			
48.44	401.2	vw, b	2352.6			
50.02	389.3	m	2364.5	$\nu_{19}+\nu_1$	e'	2365.4
50.82	383.3	w	2370.5			
51.81	375.9	w	2377.9	$\nu_6+\nu_{18}+\nu_1$;	$e'+a_1'+a_2'$	
52.40	371.5	mw	2382.3	$\nu_4+\nu_{10}+\nu_1$	e'	
3656.52	27 340.6	mw	2413.2	$\nu_{19}+\nu_{12}$	e'	2413.7
57.86	330.6	vw	2423.2	$\nu_6+\nu_{18}+\nu_{12}$	$e'+a_1'+a_2'$	
58.50	325.8	vw	2428.0	$\nu_4+\nu_{10}+\nu_{12}$	e'	
59.04	321.8	vw	2432.0	$\nu_{11}+\nu_5+\nu_1$	a_1'	
60.84	308.4	vvw, b	2445.4	?		
61.79	301.3	vw	2452.5	$\nu_{11}+2\nu_1$	a_2''	2455.4
64.49	281.2	vw, vb	2472.6	?		
65.85	273.0	vvw	2480.8	?		
65.96	270.2	vvw	2483.6	$\nu_{11}+\nu_{12}+\nu_{17}$	e'	2484.4
67.63	257.8	ms	2496.0	$\nu_6+2\nu_1$	e'	
67.83	256.3	ms	2497.5	$(\nu_8+\nu_5)$	e''	
68.71	249.7	vw	2504.1	?		
69.15	246.4	mw	2507.4	$\nu_8+\nu_{17}$ (?)	$e''+a_1''+a_2''$	2508.3
69.89	241.0	vw	2512.8			2512.4
70.49	236.6	mw, vb	2517.2	?		
71.54	228.8	vs, b	2525.0	$\nu_8+\nu_1$	e'	2525.8
72.56	221.2	vw	2532.6	?		

TABLE VII. (*Continued*)

λ_{air} (Å)	ν_{vac} (cm^{-1})	Relative intensity	$\Delta\nu$ (cm^{-1})	Assignment[a]	Vibrational symmetry in D_{3h}	Predicted harmonic value (cm^{-1})
73.46	214.5	vw	2539.1	?		
74.04	210.2	vw	2543.6	?		
3677.84	27 182.2	s	2571.6	$\nu_8+\nu_{12}$	e'	2574.1
81.34	156.3	mw, vb	2597.5	$\nu_8+\nu_1+72.0$		
82.77	145.7	vw	2608.1	$\nu_4+2\nu_1$	a_2''	2613.1
85.19	127.9	vw	2625.9	$\nu_{10}+2\nu_1$?		2632.0
86.44	118.7	vw	2635.1	$\nu_6+2\nu_{11}+\nu_1$	e'	2638.9
86.66	117.1	vw	2636.7			2639.6
87.5	111.3	w, vb	2643.5	$\nu_8+\nu_{12}+71.9$		
88.67	102.4	vvw	2651.4	?		
89.22	098.3	vvw	2655.5	?		
89.71	094.7	vvw	2659.1	?		
90.32	090.3	mb	2663.5	$\nu_8+2\nu_{11}$	e'	2664.1

[a] Brackets connect possible Fermi resonances. [b] Splitting only resolved at higher resolution.

TABLE VIII. Summary of *sym*-$C_6H_3D_3$ data (cm^{-1}).

D_{3h} symmetry class	Vibration number	Fundamental frequency			Site splitting
		Gas[a]	Liquid[a]	Crystal[b]	
a_1'	ν_1	(956)	955	954.6	
	ν_2	(3074)	(3062)	3046.3	
	ν_{12}	(1004)	1003	1002.9	
	ν_{13}	(2294)	2282	2281.4	
a_2'	ν_3	(1253)	(1252)	...	
	ν_{14}	(1321)	1322	...	
	ν_{15}	(912)	(911)	908.0[c]	
a_2''	ν_4	697	697	703.9	
	ν_5	917	918	927.8	
	ν_{11}	531	533	546.2	
e'	ν_6	594	594	591.8, 593.5	1.7
	ν_7	2282	2274	2269.0, 2274[d]	5
	ν_8	1580	1575	1571.2, 1572.2	1.0
	ν_9	1101	1101	FR	
	ν_{18}	833	833	831.5, 834.6	3.1
	ν_{19}	1414	1412	1410.8	<1
	ν_{20}	3063	3553	3060.6	<3
e''	ν_{10}	(707)	711	718.2, 722.7	4.5
	ν_{16}	(370)	375	377.5[c], 385.0[c] [378, 387]	7.5
	ν_{17}	(924)	(926)	936.6, 940.7	4.1[e]

[a] Reference 28. Values in parentheses are calculated.
[b] Not corrected for possible Fermi resonance (FR). Values in brackets are inferred from combinations.
[c] Reference 4.
[d] Frequencies for ν_7 were obtained from the fluorescence spectrum. See text.
[e] See text.

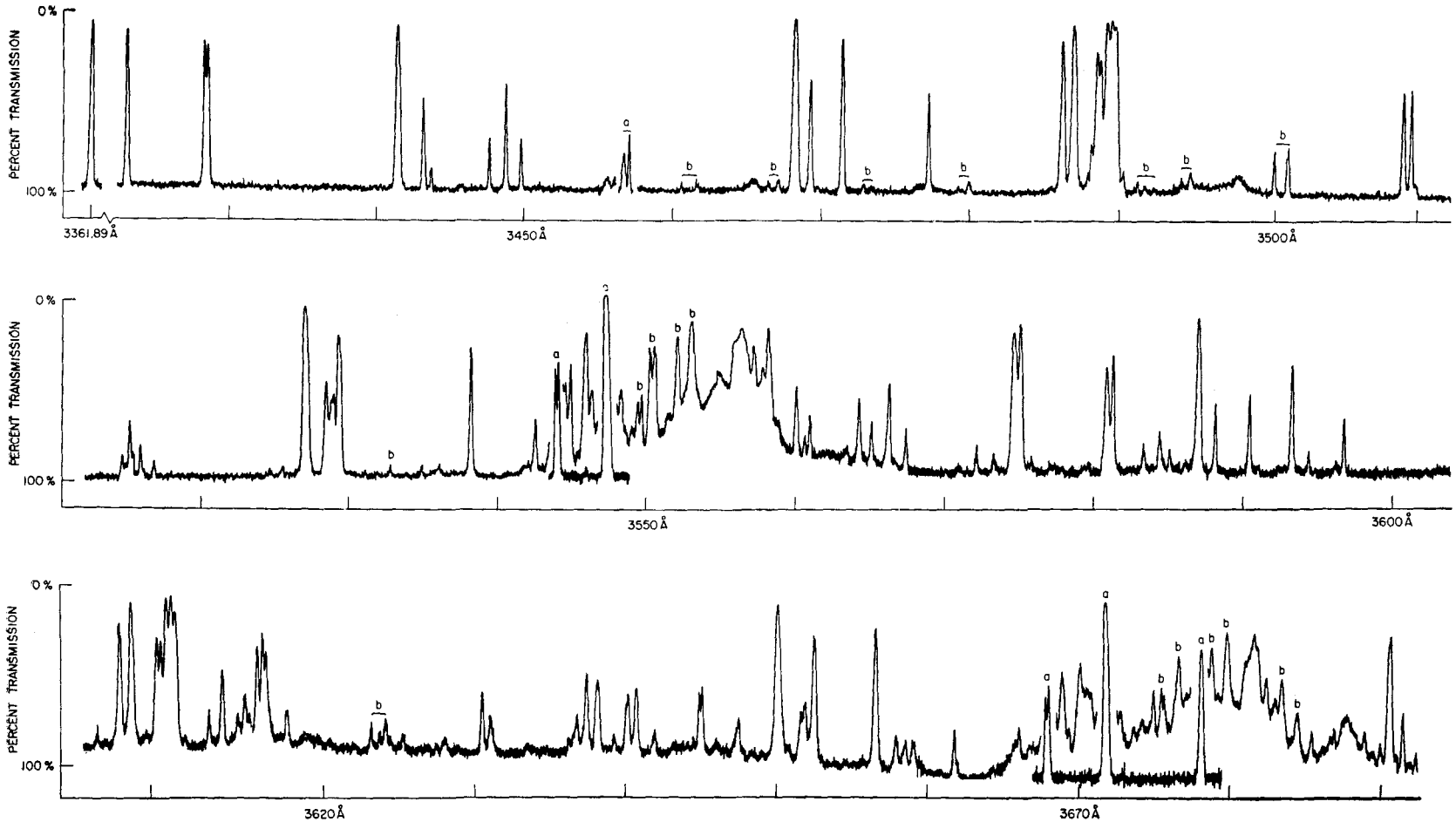

FIG. 5. Microphotometer tracing of a lower-resolution plate of the *sym*-$C_6H_3D_3$ phosphorescence. The bands labeled "a" are from a plate exposed 1/20 as long as the rest of the spectrum; "b" denotes bands assigned to *m*-$C_6H_4D_2$ and *m*-$C_6H_2D_4$ impurities.

Thus, the assignments to ν_2 and ν_{20} in the 3050-cm^{-1} region are the least certain. As seen by comparing Figs. 3 and 5, the density of lines is less in the C_6H_6 spectrum because of the higher symmetry, and these complications are therefore not so prevalent.

4. C_6H_5D

C_6H_5D has vibrational symmetry C_{2v} for a hexagonal carbon framework. As seen from the correlation diagram in Fig. 4, degenerate vibrations are split into *a* and *b* components in this lower symmetry, and all vibrations can be active in the phosphorescence spectrum. However, those vibrations that correlate directly with the more intense vibrations in the phosphorescence of C_6H_6, or those that are strongly mixed with one of these active vibrations,[28] dominate the spectrum. For example, the b_2 vibrations ν_{11} and ν_{17b} are mixed with ν_4 and ν_5, respectively. For the b_1 vibrations, strong mixing occurs among ν_{9b}, ν_{15}, and ν_{18b} and between ν_3 and ν_{14}. Thus, besides the strong vibrations corresponding to those shown in Table IV, the vibrations ν_{11}, ν_{17b}, ν_{15}, and ν_{18b} also serve as relatively strong vibronic origins of totally symmetric progressions. The weakness of the remaining vibrations again suggests that the molecular symmetry classifications are still approximately valid in the C_i site.

As a result of this mixing, the actual numbering of the fundamentals is somewhat arbitrary in a number of cases. We have generally followed Brodersen and Langseth, deviating from their labeling scheme only in one of the more arbitrary cases where the vibronic activity seemed to suggest a different assignment, i.e., ν_{9b} and ν_{15} are interchanged.

Since there are no degenerate species in point group C_{2v}, site splitting cannot occur. However, as pointed out in Sec. II, an apparently similar and related effect can and does occur. The latter has been termed the *orientation effect*.[4] The expected line pattern is given in Table I for the different isotopic modifications of benzene and for different choices of the effective site symmetry.

The phosphorescence spectrum near the electronic origin for 0.5% C_6H_5D in a C_6D_6 host crystal is shown in Fig. 6. Due to the complications of the reduced molecular symmetry and of the orientational effect, the overall density of lines is greatly increased in the C_6H_5D phosphorescence spectrum. Therefore, we have primarily concentrated on the lower-energy fundamentals and the more intense combinations. Table IX gives the complete analysis for the measured bands out to 0, $0-(\nu_{8a,b}+\nu_1)$. The electronic origin consists of a pair of lines separated by 6.5 cm^{-1} and all other vibronic bands are doublets or triplets with a total bandwidth of approximately 7 cm^{-1}. These general features have been previously described by Nieman and Tinti.[11] They assigned the 0, 0 doublet to different orientations of the guest, the 6.5-cm^{-1} "splitting"

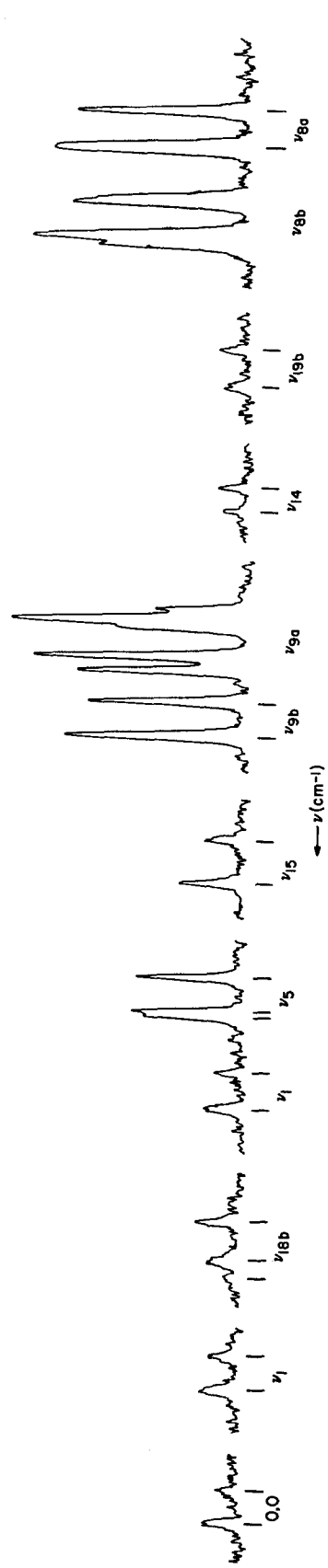

FIG. 6. Microphotometer tracing of the stronger bands of the C_6H_5D phosphorescence. The $\nu_{8a,b}$ bands are taken from a plate exposed $\frac{1}{3}$ as long as the rest of the spectrum. Lines under the trace indicate assignments.

TABLE IX. Analysis of the C_6H_5D phosphorescence.

λ_{air} (Å)	ν_{vac} (cm^{-1})	Relative intensity	$\Delta\nu$ (cm^{-1})	Assignment[a]				Vibrational symmetry in C_{2v}	Predicted harmonic value (cm^{-1})
3367.85	29 690.3	w	0	0, 0[1]	0, 0[2]				
67.11	683.8	w	6.5			0, 0[3]			
3436.53	090.8	vw, b	599.5	599.5			ν_{6a}, ν_{6b}	a_1, b_1	
37.37	083.7	vw, b	606.6			600.1			
39.14	068.8	vw, b	621.5	621.5			ν_{11}	b_2	
40.11	060.6	vw, b	629.7			623.2			
48.81	28 987.2	w	703.1	703.1			ν_4	b_2	
49.60	980.6	w	709.7			703.2			
66.88	836.1	vw	854.2	854.2					
67.23	833.2	w	857.1		857.1		(ν_{10a}), ν_{18b}	a_2, b_1	
68.15	825.6	w	864.7			858.2			
76.86	755.3	vw	937.0	937.0			ν_{17b}	b_2	
77.56	747.5	vw	942.8			936.3			
81.95	711.3	w	979.0	979.0			ν_1	a_1	
82.78	704.4	w	985.9			979.4			
84.09	693.7	w	996.6	996.6					
84.21	692.7	w	997.6		997.6		ν_5	b_2	
84.99	686.2	mw	1004.1			997.6			
3493.76	28 614.3	w	1076.0	1076.0			ν_{15}	b_1	
94.76	606.1	w	1084.2			1077.7			
3503.58	534.1	m	1156.2	1156.2			ν_{9b}	b_1	
04.39	527.5	mw	1162.8			1156.3			
05.09	521.8	mw	1168.5	1168.5				b_2	
05.43	519.0	mw	1171.3		1171.3			a_1	
06.07	513.8	w	1176.5	1176.5			ν_{9a}; $3\nu_{16}$;	b_1	
06.21	512.2	m	1178.1			1171.6	$\nu_{16}+\nu_{10}$	a_1	
07.51	510.3	w	1180.0	1180				b_2	
07.90	499.0	vw	1191.3			1184.8		b_1	
21.08	392.3	vvw	1297.5	1297.5			ν_3	b_1	
21.95	385.3	vvw	1305.0			1298.5			
23.88	369.7	vw	1320.6	1320.6			ν_{14}	b_1	
24.43	365.2	vw	1325.1			1318.4			
39.72	242.8	vw	1447.5				ν_{19b}	b_1	
40.56	236.1	vw	1454.2			1417.7			
53.27	135.0	vw, b	1555.3	1555.3			$\nu_{11}+\nu_{17b}$	a_1	1558.6
54.15	128.1	vw, b	1562.7			1555.7			1566.0

TABLE IX. (*Continued*)

λ_{air} (Å)	ν_{vac} (cm^{-1})	Relative intensity	$\Delta\nu$ (cm^{-1})			Assignment[a]	Vibrational symmetry in C_{2v}	Predicted harmonic value (cm^{-1})
3555.41	28 118.1	s	1572.2	1572.2				
55.68	115.9	s	1574.4	1574.4		ν_{8b}		
56.39	110.3	s	1580.0		1573.5	$\nu_6+\nu_1$		
56.55	109.1	s	1581.2		1574.7			
57.67	100.2	s	1590.1	1590.1				
58.52	093.5	s	1596.8		1590.3	ν_{8a}	a_1	
64.38	047.3	vw, b	1643.0			$\nu_{8b}+69.7$		
66.52	030.5	vw, b	1659.8			$\nu_{8a}+69.7$		
69.31	008.6	w	1681.7	1681.7				1682.1
70.19	001.7	w	1689.6		1683.1	$\nu_4+\nu_1$	b_2	1689.1
81.91	27 910.1	vw	1780.2	1780.2				
82.57	905.0	vw	1785.3		1778.8	$(\nu_{10b}+\nu_1)$	b_2	
89.19	853.5	vw, b	1836.8	1836.8				1833.2
90.13	846.2	vw	1844.1		1837.6	$\nu_{18b}+\nu_1$	b_1	1836.1 1844.1
99.29	775.4	vw	1914.9	1914.9				1916.0
3600.21	768.3	vw	1922.0		1915.5	$\nu_{17b}+\nu_1$	b_2	1922.0
04.73	733.4	vw	1956.9	1956.9				1958.0
05.68	726.1	vw	1964.2		1957.3	$2\nu_1$	a_1	1965.3
3607.12	27 715.0	w	1975.3	1975.3				1975.6
07.25	714.0	w	1976.3		1976.3			
08.09	707.6	w	1982.7		1975.7	$\nu_5+\nu_1$	b_2	1976.6 1983.5
17.50	635.5	vw	2054.8	2054.8				2055.0
18.62	627.0	vw	2063.3		2056.8	$\nu_{15}+\nu_1$	b_1	2063.6
28.03	555.3	m	2135.0	2135.0				2135.2
28.92	548.6	mw	2141.7		2135.2	$\nu_{9b}+\nu_1$	b_1	2142.2
29.67	542.9	mw	2147.4	2147.4				
30.04	540.1	m	2150.2		2150.2	$\nu_{9a}+\nu_1$;		
30.86	533.9	vw	2156.4			$3\nu_{16}+\nu_1$;		
30.95	533.2	m	2157.1		2149.2	$\nu_{16}+\nu_{10}+\nu_1$		
31.30	530.5	vw	2159.8					
49.54	392.9	vvw	2297.4	2297.4		$(\nu_3+\nu_1)$, ν_{7a}	b_1	
49.87	390.4	vw	2299.9	2299.9				2299.6
50.38	386.6	vw	2303.7		2297.7	$\nu_{14}+\nu_1$	b_1	2304.3
66.64	265.0	vw	2425.3	2425.3				2426.5
67.60	258.1	vw	2432.2		2425.7	$\nu_{19b}+\nu_1$	b_1	

TABLE IX. (*Continued*)

λ_{air} (Å)	ν_{vac} (cm^{-1})	Relative intensity	$\Delta\nu$ (cm^{-1})		Assignment[a]	Vibrational symmetry in C_{2v}	Predicted harmonic value (cm^{-1})
83.06	143.6	s	2546.7	2546.7			
83.34	141.5	s	2548.8		2548.8 $\nu_{8b}+\nu_1$	b_1	
84.18	135.3	s	2555.0		2547.5 $\nu_6+2\nu_1$	b_1, a_1	
3686.20	27 120.5	s	2569.8	2569.8			2569.1
87.18	113.3	s	2577.0		2570.5 $\nu_{8a}+\nu_1$	a_1	2582.7

[a] Brackets connect possible Fermi resonances.

representing the difference in zero-point energies among distinct guest molecules with different orientations of the molecular twofold axis in the nearly C_{2h} site. Thus, based on each component of the 0, 0 band, vibronic lines appear with energy separations corresponding to vibrational frequencies.

For example, consider the doublet assigned to 0, 0$-\nu_1(a_1)$ in Fig. 6. Each of these represents the subtraction of a quantum of the totally symmetric mode ν_1 from its respective 0, 0 line. Nieman and Tinti[11] have been able to show from concentration studies that for some of the more intense lines, the high-energy member of a vibronic doublet corresponds to the high-energy member of the 0, 0 band. In the analysis for ν_1 presented in Table IX, the subtractions are made assuming this correlation to hold. Two values are obtained for ν_1, 979.0 and 979.4 cm^{-1}. The difference in these two values results from the nonequivalence of the guest–host interactions when different guest molecules undergo the same vibration in two physically different orientations. The 0.4-cm^{-1} difference between the two ν_1 vibrational frequencies is the orientational effect on this vibration for C_6H_5D in a C_6D_6 host crystal. If this vibration were observed with sufficient resolution in the infrared or by the Raman effect, it would appear as a close doublet with a splitting of 0.4 cm^{-1}. Orientational splittings have indeed been observed in certain infrared transitions and will be the subject of a future paper.[4a] The full 6.9-cm^{-1} splitting between the two observed lines in the phosphorescence spectrum contains, besides this vibrational orientational contribution, an orientational contribution to the zero-point energies in the two electronic states.

Since the crystallographic site symmetry is C_i and not C_{2h}, triplets are predicted instead of the generally observed doublets. In fact, triplets are actually observed for some bands, e.g., ν_{18b} and ν_5 in Fig. 6, and they may be inferred in others since the high-energy member of the doublet appears itself like an unresolved doublet. Because of this, and in addition to the concentration studies of Nieman and Tinti, two of the three electronic origins are assigned to the higher-energy component of the 0, 0 band. In Table IX the two members of this nearly degenerate pair are designated as 0, 0^1 and 0, 0^2; the third origin 6.5 cm^{-1} to lower energy is called 0, 0^3.

For the vibronic bands that appear as doublets, the vibrational energy quantum corresponding to origins 0, 0^1 and 0, 0^2 are again nearly degenerate. If the vibronic band is a triplet, the two lines at higher energy are subtracted from the assumed degenerate electronic origins 0, 0^1 and 0, 0^2 to obtain the respective vibrational quantum for these two guest orientations. The vibrational energy in the third orientation is obtained by subtracting the low-energy line of the triplet vibronic band from 0, 0^3. In this fashion, three different frequencies are generally obtained for these vibrational modes as shown in Table IX.

The results are summarized in Table X, which gives all the directly observed fundamental frequencies together with their orientational effects. The near equivalence of the 0, 0^1 and 0, 0^2 orientations is demonstrated by the fact that only two of the 15 observed fundamentals show a triplet structure and thus have nonzero entries in Column 6 of Table X. This indicates that the effective site symmetry is very nearly C_{2h}. The effect of orientation on the vibrational energy in the two cases showing the triplet structure is quite large. It should be noted that both positive and negative energy shifts are observed for the orientational effect. In those instances where the fundamentals reported here are observed directly in the infrared the agreement is excellent. No orientation effect has been reported for ν_{9a} or ν_{8b} as it is difficult to assign conclusively all the lines in these regions of the spectrum. It appears that these fundamentals are in Fermi resonance with combinations (see Table IX).

Since the orientational effects are small, it is neces-

TABLE X. Summary of C_6H_5D data (cm^{-1}).

C_{2v} symmetry class	Vibration number	Gas[a]	Liquid[a]	Crystal sites 1	2	3	Orientational effect 2–1	3–2	Comments[b]
a_1	ν_1	(983)	(983)	979.0		979.4		+0.4	
	ν_{8a}	(1600)	1593	1590.1		1590.3		+0.2	FR: ν_{8a}, ν_{8b}, and $(\nu_6+\nu_1)$
	ν_{9a}	(1177)	1177	1171		...	...	...	FR: $(\nu_{10}+\nu_{16b})$ and $3\,\nu_{16b}$; F
b_1	ν_8	(1295)	1291	1297.5		1298.5	0	+1.0	
	ν_{6b}	(607)	602	599.5		600.1	0	+0.6	ν_{6a} and ν_{6b} in resonance
	ν_{8b}	(1590)	1576	1575.2		...	0		FR: ν_{8a}, ν_{8b} and $(\nu_6+\nu_1)$; F
	ν_9	(1157)	1158	1156.2		1156.3	0	+0.1	
	ν_{14}	(1327)	(1325)	1320.6		1318.4	0	−2.2	
	ν_{15}	1077	1077	1076.0		1077.7	0	+1.7	
	ν_{18b}	858	857	854.2	857.1	858.2	+2.9	+1.1	FR: ν_{10a}
	ν_{19b}	1440–1490	1448	1447.5		1447.7	0	+0.2	FR: ν_{19a}
b_2	ν_4	698	699	703.1		703.2	0	+0.1	
	ν_5	(984)	978	996.6	997.6	997.6	+1.0	0	
	ν_{11}	607	602	621.4		623.6	0	+2.2	FR: ν_6 in liquid
	ν_{17}	924	925	937.0		936.3	0	−0.7	

[a] Reference 28. Parentheses indicate calculated values. [b] FR is Fermi resonance; F is frequency observed in the fluorescence.

sary to analyze carefully the sources and the magnitudes of the errors in obtaining the final result. The first consideration is the validity of the subtractions. These have been made subject to two restrictions. The concentration studies of Nieman and Tinti, as mentioned earlier, allow the relative intensities of the three orientational components to be varied. The reason for this variation is that the relative populations of the initial states for the emission process can be changed through excitation transfer among the three sets of differently oriented molecules. The efficiency of excitation transfer increases with concentration of guests. It is therefore generally a straightforward matter to distinguish for all vibronic transitions site 3 from the other two sites by concentration variations. However, it should be noted that the concentration studies did not include all the vibrations listed in Tables IX and X. The second consideration in making these subtractions is that orientation effects are expected to be small,[4] so certain assignments are favored over others that give large orientation effects. On top of the uncertainties about making the subtractions, experimental errors can distort the final results. This factor leads to an uncertainty in the orientational effect of $\lesssim 0.5$ cm^{-1}. The relatively large error is a consequence mainly to the three differences involved and round-off error in the absolute energy of any given vibronic line, which is reported only to ± 0.1 cm^{-1}.

5. *p*-$C_6H_4D_2$

For *p*-$C_6H_4D_2$, which has vibrational symmetry D_{2h} for a hexagonal carbon framework, the correlation diagram in Fig. 4 shows that the *g* vibrations a_{1g}, b_{1g}, and b_{3g} can be group-theoretically active in the phosphorescence spectrum. Besides those vibrations that correlate directly with the more active vibrations of C_6H_6, a significant activity is also seen of the vibrations $\nu_{10b}(b_{3g})$ and $\nu_3(b_{2g})$, which mix with $\nu_4(b_{3g})$ and $\nu_{9b}(b_{2g})$, respectively. As in C_6H_5D, no degeneracies remain in the vibrational manifold of *p*-$C_6H_4D_2$. However, inversion symmetry is preserved in the latter isotope so that the same fundamentals are not observed in the infrared and the electronic emission spectra.

As can be seen from the phosphorescence spectrum of 0.5% *p*-$C_6H_4D_2$ shown in Fig. 7, the electronic 0, 0 transition and many other vibronic bands are resolved triplets. Because of the complex nature of this spectrum, it was not completely analyzed. A partial analysis of the spectrum is given in the figure, where the average bandwidth of the triplets is about 13 cm^{-1}, about double that of C_6H_5D. The origin of the electronic splittings and their relative magnitude for various isotopes have

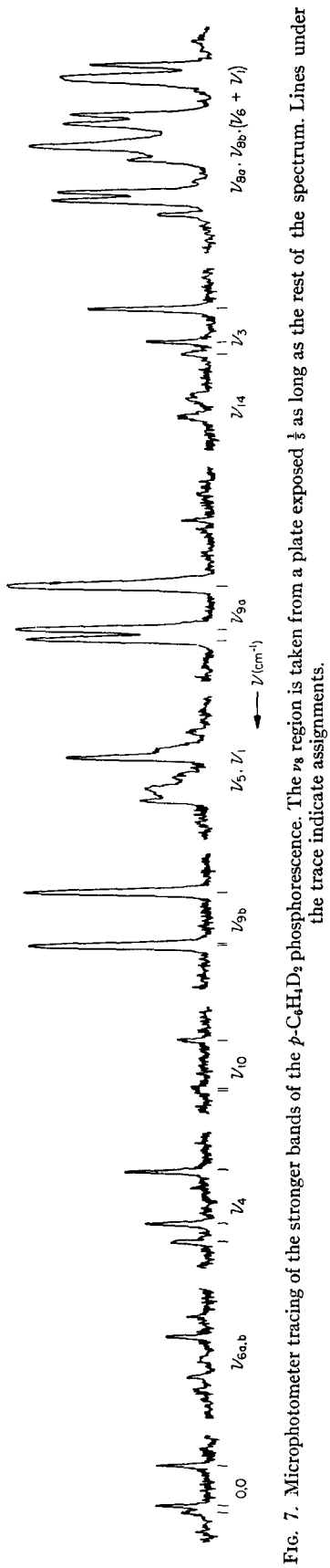

FIG. 7. Microphotometer tracing of the stronger bands of the p-$C_6H_4D_2$ phosphorescence. The ν_8 region is taken from a plate exposed $\frac{1}{5}$ as long as the rest of the spectrum. Lines under the trace indicate assignments.

been discussed previously.[11] Proceeding as in C_6H_5D, three different frequencies corresponding to 0, 0^1, 0, 0^2, and 0, 0^3 exist for each vibrational mode. The vibrations given in Table XI, however, are the only ones for which an unambiguous assignment of the orientation effect could be made.

V. $^1B_{2u}$—$^1A_{1g}$ ABSORPTION SPECTRA

The vibronic absorption spectrum of the guest in an isotopic mixed crystal also provides a useful tool for studying the effects of the crystal environment on the molecular energy levels. Not only can some excited-state vibrations be studied, but the orientational structure of the 0, 0 band can be observed directly. Guest singlet←singlet absorption spectra can be very sharp in properly prepared crystals, but care must be exercised to avoid straining the crystal if maximum sharpness is to be obtained.[29] In the thicker crystals of C_6H_6 in C_6D_6, absorption linewidths as narrow as 0.6 cm^{-1} have been measured. The structure of the guest 0, 0 absorption transition is given in Table XII for mixed crystals of C_6H_6, C_6H_5D, p-$C_6H_4D_2$, and *sym*-$C_6H_3D_3$ at concentrations $\lesssim 0.005\%$ in a C_6D_6 host at 4.2°K. The doublet structure for the molecules of lower symmetry represents the differences in the orientational effects of the ground and lowest excited singlet states, including both the vibrational contribution to zero-point energies and any electronic effect. From a comparison of Tables IX, XI, and XII, one can see that the electronic orientational splittings for the $^1B_{2u}$←$^1A_{1g}$ transition are about $\frac{1}{5}$ those for the $^3B_{1u}$→$^1A_{1g}$ transition, but in both transitions the over-all splitting for p-$C_6H_4D_2$ is about twice that for C_6H_5D. For a detailed discussion of the significance of these differences, see Nieman and Tinti.[11]

Fairly thin crystals (~20 μ) are required for observation of the higher vibronic guest transitions, as such absorptions are completely masked by the host absorption in the thick samples. The vibrational frequencies obtained from these absorption lines are less significant than those of ground-state vibrations as excited-state levels are more apt to be shifted by interactions with the host. The excitation exchange interactions are typically larger for the singlet vibronic bands than for the ground-state vibrational bands and thus quasiresonance interactions[30] with nearby host bands could cause a different shift in each vibronic level. A few mixed crystal transitions of C_6H_6 are given in Table XIII from which it can be seen that the ν_6' site splitting (2.1 cm^{-1}) is less than that for ν_6'' (3.1 cm^{-1}). This splitting should not necessarily be the same as that for ν_6' in a pure C_6H_6 crystal, which has been reported[31] to be 9 cm^{-1}, since resonance interactions must contribute to the splitting in the pure crystal.

[29] S. D. Colson, J. Chem. Phys. **45**, 4746 (1966).
[30] G. C. Nieman and G. W. Robinson, J. Chem. Phys. **38**, 1928 (1963).
[31] V. L. Broude, Usp. Fiz. Nauk **74**, 577 (1961) [Sov. Phys.—Usp. **4**, 584 (1962)].

TABLE XI. Summary of p-$C_6H_4D_2$ data (cm^{-1}).

D_{2h} symmetry class	Vibration number	Gas[a]	Liquid[a]	Crystal sites 1	2	3	Orientational effect 2-1	3-2
	0, 0			29 721.4	29 719.5	29 708.0	−1.9	−11.5
b_{3g}	ν_4	(633)	633	637.9	641.2	643.6	+3.3	+2.4
	ν_{10b}	(739)	736	744.3	742.4	742.9	−1.9	+0.5
	ν_3	(1307)	1311	1 310.2	1 311.5	1 308.1	+1.3	−3.4
a_{1g}	ν_{9a}	(1177)	1173	1 171.4	1 172.9	1 171.8	+1.5	−1.1
b_{2g}	ν_{9b}	(913)	908	908.4	906.5	909.1	−1.9	+2.6

[a] Reference 28. Parentheses indicates calculated values.

Absorptions due to benzene containing ^{13}C in natural abundance have also been observed (see Table XII). In thick crystals with about 0.04% C_6H_6, considerable fine structure surrounding the 0, 0 line is seen at high spectral resolution. The spectrum is shown in Fig. 8 and analyzed in Table XIV. The fine structure components are tentatively assigned to $^{13}C_1$ benzene, $^{13}C_2$ benzene, and to pairs of guest molecules in adjacent sites ("dimers" or "resonance pairs"). The line at 37 856.9 cm^{-1} is assigned to $^{13}C_1$ benzene because of the presence of a 982-cm^{-1} (ν_1, a_1) progression built on this origin in the $^1B_{2u} \rightarrow {}^1A_{1g}$ emission spectrum, as described earlier, and on its intensity relative to the $^{12}C_6H_6$ 0, 0 absorption. The $^{13}C_2$-benzene assignment is made from an analogy with the deuterium isotope effect[11,23]; that is, the $^{13}C_2$ line is expected to be shifted twice as much as the $^{13}C_1$ line. Also in analogy with the deuterium effect, the o-, m-, or p- $^{13}C_2$ shifts are expected to be nearly equal (within 10% of one another). The assignment of the line at 37 848.6 cm^{-1} to a resonance pair is made on the basis of its concentration dependence; that is, its intensity decreases more rapidly than that of the C_6H_6 "monomer" absorption with decreasing C_6H_6 concentration. The line at 37 851.2 cm^{-1}, which may also be due to one line of a resonance pair, has not been shown to have the expected concentration dependence. However, its intensity may be anomalous because it is too near the intense monomer absorption. No evidence has yet been obtained for the resonance pair spectra from emission spectra, but no great effort has been made to search for them there.

At the highest resolution employed, additional absorption lines very near the monomer line are resolved. These are given in Table XIV, but are unresolved in the

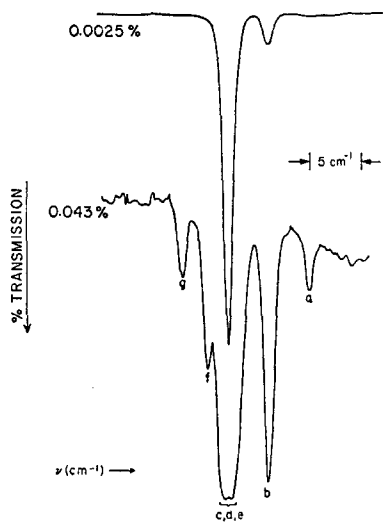

FIG. 8. Microphotometer tracing of the C_6H_6 electronic origin at two concentrations in a 2-mm-thick C_6D_6 host crystal. See Table XIII for the frequencies.

TABLE XII. $^1B_{2u} \leftarrow {}^1A_{1g}$ electronic transition energy for isotopic guests at infinite dilution in a C_6D_6 host crystal at 4.2°K.

	Mixed crystal[a] (cm^{-1}) $^{12}C_6H_nD_{6-n}$	Mixed crystal[a] (cm^{-1}) $^{13}C^{12}C_5H_nD_{6-n}$	Gas[b] (cm^{-1}) $^{12}C_6H_nD_{6-n}$
C_6H_6	37 853.3	37 856.9	38 086.1
C_6H_5D	37 885.2	37 888.8	38 124
	37 884.0	37 887.7	
p-$C_6H_4D_2$	37 915.7		38 154
	37 912.9		
sym-$C_6H_3D_3$	37 947.9	37 951.4	38 184

[a] Uncorrected for interaction with the C_6D_6 host. The ^{12}C guest is present at $\lesssim 0.005\%$; the corresponding ^{13}C guest concentration is natural abundance.

[b] The C_6H_6 value is from Ref. 19. For the other isotopes the 0, 0 is taken from Ref. 23.

TABLE XIII. Partial analysis of the $^1B_{2u}\leftarrow{}^1A_{1g}$ absorption spectrum of C_6H_6 in a C_6D_6 host crystal at 4.2°K.

λ_{air}	ν_{vac}	$\Delta\nu$	Assignment	Gas $\Delta\nu$
2641.00	37 853.3	0	0-0	
2605.34	38 371.3	518.0	ν_6'	522.4[a]
2605.20	38 373.4	520.1		
2577.89	38 779.8	926.5	ν_1'	923[b]
2543.9	39 297	1444	$\nu_1'+\nu_6'$	

[a] Reference 19.
[b] F. M. Garforth and C. K. Ingold, J. Chem. Soc. 1948, 417.

lower-resolution spectrum shown in Fig. 8. Their concentration dependence and, therefore, their definite assignment is unknown. Similar lines were seen for the other deuterated isotopes. The C_6H_5D data are also given in Table XIV; note the orientational splittings of a number of the lines.

It should be pointed out that polarized absorption spectra of resonance pairs of molecules in isotopic mixed crystals allow the magnitudes and relative signs of pairwise intermolecular excitation exchange interactions to be determined directly. Such experiments therefore may be quite important in the interpretation of the pure crystal spectrum.

VI. DISCUSSION AND CONCLUSIONS

From the results presented in the summary tables, both site splittings and orientational effects are seen to be a general occurrence in the benzene crystal. The magnitude of the effects are generally insensitive to isotopic substitution or *g*- or *u*-symmetry classification. The effects are greatly sensitive to vibration type only when comparing in-plane and out-of-plane vibrations. Even the gas-to-crystal frequency shifts follow this general pattern. Apparent exceptions for the site shifts are the particular in-plane vibrations ν_2, ν_7, ν_8, and ν_{13}. The anomalously large gas-to-crystal shifts for these particular vibrations parallel large gas-to-liquid shifts, while for the other fundamentals the gas-to-liquid shifts are very small. The average site shift for the other in-plane vibrations is very nearly zero and certainly lies within the combined gas and crystal experimental frequency error (2—3 cm^{-1}). For the out-of-plane vibrations the average solid–gas site shift is greater than 10 cm^{-1}.

The same trend is followed in the site splittings (see Tables IV and VIII). The average site splitting for out-of-plane vibrations is $\sim$7 cm^{-1} while the in-plane vibrations have an average site splitting of roughly 3 cm^{-1}. For the orientational effect, the distinction between in-plane and out-of-plane bands is less clear and it appears that the effect is more dependent on the particular vibrational mode. We note, however, that for $\nu_{16}(CC^{\perp})$ the orientational effect as seen in the infrared[4] in C_6H_5D and *p*-$C_6H_4D_2$ is the largest observed. Furthermore, the average maximum splitting among the orientational components is generally less than the site splitting.

We suggest that the distinction between in-plane and out-of-plane modes is probably due to the greater vibrational amplitude for the out-of-plane displacements. This could imply that interaction with the crystal environment for the out-of-plane modes is greater and, therefore, larger site shifts, site splittings, and orientational effects result.

The site splitting observed in the fundamental ν_6 for C_6H_6 is 3.1 cm^{-1}. When totally symmetric additions $\nu_6+n\nu_1$ are made, these levels come into Fermi resonance with $\nu_8+(n-1)\nu_1$, and the measured splitting decreases to roughly 1.2 cm^{-1} as shown in Table XV. The assignment of the "ν_6 component" in the Fermi doublet is made by comparison of the intensities of the members of the Fermi couple with the ν_6 fundamental in the fluorescence and phosphorescence emissions (cf., Table III and Fig. 2). The decrease in the measured splitting of ν_6 for C_6H_6 in the Fermi couple is apparently due to the resonance. Note, however, that the "lost splitting" does not appear in the other half of the couple ν_8. In *sym*-$C_6H_3D_3$ this same resonance does not appear to be as strong since the observed value for $\nu_6+\nu_1$ is closer to the harmonic value. The *sym*-$C_6H_3D_3$ site splitting in the progression $\nu_6+n\nu_1$ is more nearly constant and equals 1.7, 1.9, and 1.5 cm^{-1} for $n=0$, 1, and 2, respectively. Furthermore, ν_8 is split by 1.0 cm^{-1}. See Table VII.

Even though the site-split components of a degenerate fundamental usually have very nearly equal vibronic intensities, the fundamentals ν_{10} in both C_6H_6 and *sym*-$C_6H_3D_3$ and ν_{17} in *sym*-$C_6H_3D_3$ are exceptions. Exactly how to evaluate this difference in vibronic intensities is not clear at present. Mixing and Fermi resonance among the components can contribute to the site splitting and, if substantial, these interactions would tend to equalize the vibronic intensities. Therefore, one might conclude that for the bands where significant intensity differences are seen, such intrasite interactions are small. The inverse, however, need not be true; that is, nearly equal intensities of the site components do not necessarily imply strong intrasite interactions. It may just be that in these cases the site-split components are equally good "intensity stealers". In combination and overtone bands the relative intensity of the components is variable. For example, the components of $(\nu_{16}+\nu_{11})$ and $2\nu_{16}$ in C_6H_6 show a "normal" intensity pattern in the phosphorescence, but in the fluorescence, the $2\nu_{16}$ triplet deviates from the

TABLE XIV. Structure observed near the electronic origin for C_6H_6 and C_6H_5D at higher concentrations in a C_6D_6 host at 4.2°K.

	C_6H_6[a]			C_6H_5D[a]		
	ν (cm^{-1})	I	Assignment	ν (cm^{-1})	I	Assignment
a[b]	37 860.9	w	$^{13}C_2{}^{12}C_4H_6$	37 892.5 37 891.6	w w	$^{13}C_2{}^{12}C_4H_5D$
b	37 856.9	s	$^{13}CC_5H_6$	37 888.8 37 887.7	s s	$^{13}C^{12}C_5H_5D$
c	~37 854.1	w, sh		...		
d	37 853.3	vs	Monomer	37 885.2 37 884.0	vs vs	Monomer
e	37 852.3	w		...		
f	37 851.2	w		37 882.7	w	
				37 881.8	w	
g	37 848.6	w	Resonance pair	37 880.0	w, b	Resonance pair

[a] 0.04% guest in a ~2-mm C_6D_6 host crystal. [b] See Fig. 8.

expected 1:2:1 ratio, whereas $(\nu_{11}+\nu_{16})$ again appears as a normal doublet. Other examples are evident both from the approximate intensities given in Tables III and VII and from Figs. 2 and 5 and were discussed in earlier parts of this paper.

TABLE XV. Change in the C_6H_6 1600-cm^{-1} ν_8 and $\nu_6+\nu_1$ Fermi couple splitting with totally symmetric ν_1 additions.

n	$\nu_8+(n-1)\nu_1$ (cm^{-1})	$\nu_6+n\nu_1$ (cm^{-1})	Site splitting (cm^{-1})	Fermi splitting (cm^{-1}) Solid[a]	Gas[b]
0	...	606.3 609.4	3.1	...	...
1	1584.3	1602.8 1604.0	1.2	19.1	20
2	2568.1	2594.3 2595.5	1.2	26.8	26
3	3551.6	3583.5 3584.8	1.3	32.5	31
4	4534.1	4571.5[c]		37.4	37

[a] The mean of the two $\nu_6+n\nu_1$ site components is used to calculate the Fermi splitting.
[b] F. M. Garforth, C. K. Ingold, and H. G. Poole, J. Chem. Soc. **1948**, 427.
[c] This band is too weak to observe any splitting.

One would also expect an increased mixing and interaction among different molecular vibrations in the crystal relative to the free molecule. These effects are expected to show up most clearly where they are symmetry forbidden or weak in the molecule but allowed in the crystal site. For example, in the case of $\nu_6+n\nu_1$ interacting with $\nu_8+(n-1)\nu_1$, given in Table XV, crystal effects are obviously small. However $\nu_{16}+\nu_{10}$ interacting with ν_9 (see Fig. 5 and Table VII, and ν_{20} interacting with ν_2 in sym-$C_6H_3D_3$ seem to be examples of crystal-site-induced interactions.

A further possible indication of the magnitude of crystal-site effects can be obtained from anharmonicities. Observing $n\nu_1$ out to $n=5$ in the C_6H_6 fluorescence, the anharmonic effects are seen to be small as they are in the gas phase.[23] The only other vibrations whose overtones are observed are ν_{16} and ν_{10}, but in these cases Fermi resonance in the crystal site among the three components of the overtone complicates the analysis of the anharmonicities. Similar difficulties are encountered in the combination bands.

The general conclusion from the gross vibrational structure is that neither the frequencies nor the symmetry classifications of the vibrations are strongly perturbed by the crystal. This is specifically shown by the small magnitude of the site shifts, splittings, and orientational effects and by the dominance of the e_{2g} vibrations in the singlet and triplet spectra. The most pronounced effect of the crystal is the appearance of the 0, 0 progressions in the two emissions.